

HSMA_WOA: a hybrid novel Slime mould algorithm with whale optimization algorithm for tackling the image segmentation problem of chest X-ray images

Mohamed Abdel-Basset¹, Victor Chang² and Reda Mohamed¹

¹ Faculty of Computers and Informatics, Zagazig University, Sharqiyah, Egypt.

E-mails: analyst_mohamed@zu.edu.eg; redamoh@zu.edu.eg

² School of Computing, Engineering and Digital Technologies, Teesside University, UK

Email: victorchang.research@gmail.com/V.Chang@tees.ac.uk

*Correspondence: Victor Chang; Email: victorchang.research@gmail.com/V.Chang@tees.ac.uk

Abstract

Recently, a novel virus called COVID-19 has pervasive worldwide, starting from China and moving to all the world to eliminate a lot of persons. Many attempts have been experimented to identify the infection with COVID-19. The X-ray images were one of the attempts to detect the influence of COVID-19 on the infected persons from involving those experiments. According to the X-ray analysis, bilateral pulmonary parenchymal ground-glass and consolidative pulmonary opacities can be caused by COVID-19 - sometimes with a rounded morphology and a peripheral lung distribution. But unfortunately, the specification or if the person infected with COVID-19 or not is so hard under the X-ray images. X-ray images could be classified using the machine learning techniques to specify if the person infected severely, mild, or not infected. To improve the classification accuracy of the machine learning, the region of interest within the image that contains the features of COVID-19 must be extracted. This problem is called the image segmentation problem (ISP). Many techniques have been proposed to overcome ISP. The most commonly used technique due to its simplicity, speed, and accuracy are threshold-based segmentation. This paper proposes a new hybrid approach based on the thresholding technique to overcome ISP for COVID-19 chest X-ray images by integrating a novel meta-heuristic algorithm known as a slime mould algorithm (SMA) with the whale optimization algorithm to maximize the Kapur's entropy. The performance of integrated SMA has been evaluated on 12 chest X-ray images with threshold levels up to 30 and compared with five algorithms: Lshade algorithm, whale optimization algorithm (WOA), FireFly algorithm (FFA), Harris-hawks algorithm (HHA), salp swarm algorithms (SSA), and the standard SMA. The experimental results demonstrate that the proposed algorithm outperforms SMA under Kapur's entropy for all the metrics used and the standard SMA could perform better than the other algorithms in the comparison under all the metrics.

Keywords: Image segmentation problem; Slime mould algorithm(SMA); whale optimization algorithm; Kapur's entropy; X-ray images; COVID-19.

1. Introduction

Starting in China and passing to all the worldwide, a novel virus named COVID-19 outbreaks continuously. This virus infects the victim with fever and respiratory symptoms such as cough and sore throat. However, those symptoms do not confirm the infection with COVID-19 [1], so many attempts have

been performed to find a tool that confirms if the person infected with COVID-19. After making chest CT imaging for suspects infected with COVID-19, the bilateral pulmonary parenchymal ground-glass and consolidative pulmonary opacities can be used to determine the infection. A rounded morphology and a peripheral lung distribution could sometimes be spotted [2].

Fortunately, since the CT findings are extracted as a normal image, it could be segmented into similar small regions, some of which may contain the features of COVID-19. The process of segmenting an image is commonly known as an image segmentation problem (ISP) and many algorithms have been applied for overcoming ISP. However, those algorithms still suffer from some problems prevent from reaching better-segmented images. As a result, the need for a new robust algorithm to segment the images has significantly been increased those days, especially with appearing chest CT images.

Recently, a novel algorithm known as the slime mould algorithm (SMA) inspired the slime mould behaviors to obtain the optimal track for gathering food. SMA has already been proposed for tackling the continuous optimization problems and could achieve significant success in comparison with the other algorithms. Accordingly, in this paper, SMA is adopted to tackle the chest X-ray image segmentation problem for the first time, as a new addition to separate the similar regions or to extract the region of interest inside an X-ray image. In addition, as an attempt to improve the performance of SMA and proposing a multi-thresholding model has a high ability on tackling ISP, the whale optimization algorithm (WOA) will be integrated with it to borrow its exploration capability within the first half of the iterations and after finishing the predefined first iterations where WOA runs within, the SMA will start to exploit around the best region explored by WOA with disposing of local minima problem under its ability that will re-initialize the solutions within the search space under a certain probability. The proposed model is only observed on X-ray test images infected with COVID-19, so it is proposed for dealing with this type of image. And within our future work, its performance will be validated on a number of test images from The Berkeley Segmentation Dataset and Benchmark to see if its performance is stable on any image or not.

The contribution of this paper is summarized as follows: First, a new integrated approach (HSMA_WOA) is proposed based on the behavior of SMA and WOA for finding the optimal threshold values that overcome the multi-threshold image segmentation problems of chest X-ray images. Second, experiments of HSMA_WOA have been undertaken and outperforming all the compared algorithms in fitness values, PSNR, UQI, SSIM, CPU time, and standard deviation under Kapur's entropy.

The rest of this paper is structured as follows. In section 2, some proposed works for ISP has been reviewed. Additionally, Kapur's entropy is explained in Section 3. Sections 4 and 5 give a description of the whale optimization algorithm, and the slime mould algorithm, respectively. Section 6 introduces the proposed work for overcoming the image segmentation problem. Section 7 illustrates the results obtained under both Kapur's and entropy functions. Finally, section 8 concludes the paper.

2. Related work

Nowadays, ISP plays a crucial role in image processing [3] and computer vision [4] to focus on an interesting region rather than the whole image until managing to analyze the image with higher accuracy. ISP is present in many fields such as medical diagnosis [5, 6], object recognition [7], satellite image processing [8], remote sensing [9], historical documents [10], and historical newspapers [11, 12].

Several methodologies for tackling ISP, such as region-based [13], edge-based [14], feature selection-based clustering [15], and threshold-based [16], has been suggested to help in separating the similar regions into an image. From involving those methodologies, Threshold-based segmentation is deemed the best one for solving the ISP [3, 17, 18]. Due to its simplicity, speed, and accuracy compared with the others. Thresholding is classified into two types: a bi-level threshold and a multi-level threshold. If the image contains only two similar regions: object and background, then the bi-level threshold is the best candidate for separating those two regions; otherwise, the multi-level threshold is better. Although the multi-level threshold could help in segmenting the image with more than two regions, the time increases exponentially when the number of regions increases.

Some techniques proposed for solving the image segmentation problem are based on an approach that needs to identify some parameters for each class using a probability density function for segmenting the image, those approaches are classified as parametric [19]. Meanwhile, another approach classified as non-parametric [19] maximizes a function (such as Kapur’s entropy [20], fuzzy entropy [21], and Otsu function) without needing to calculate parameters at the outset.

Due to the time complexity problem with the increased threshold levels, traditional techniques failed to be the best tool for solving the ISP. Subsequently, the need for another different technique to overcome the problem of time complexity was significantly increased. Thus, the meta-heuristic algorithms (MHAs) have been more popular among researchers since significant superiorities with less time in several fields were offered by MHAs [22-27] as the most appropriate tool to solve the ISP and overcome the time complexity. Since the w processing time increases exponentially with increasing thresholds, traditional techniques will use the considerable time to search for the optimal threshold.

Recently, many meta-heuristic algorithms have been suggested for overcoming ISP, such as particle swarm optimization (PSO) [28-30], ant-colony optimization algorithm [31], bee colony algorithm (BCA) [32], whale optimization algorithm (WOA) [33], genetic algorithm (GA) [34], multi-verse optimizer [35], cuckoo search (CS) [36], symbiotic organisms search (SOS) [37], Harris hawks optimization algorithm (HHA) [38], and firefly optimization algorithm (FFA) [39], flower pollination algorithm (FPA) [40], crow search algorithm [41], grey wolf optimizer [42], honey bee mating (HBM) optimization [43], locust search algorithm (LSA) [44], moth-flame optimization algorithm (MFA) [33], and firefly optimization algorithm (FFA) [39]. Some of those algorithms are summarized in the following Table.

Table 1: Some algorithms proposed for solving ISP

	Reference	Procedure
1	Singla and Patra [45]	The cluster validity measure was used to investigate the boundaries of the threshold levels to find the bounds that may contain the optimal threshold values. Then, it applied GA on the obtained bounds to search for the optimal threshold values within.
2	Manikandan et al. [46]	The real coded GA with the simulated binary crossover has been suggested for tackling the ISP of the medical image by maximizing the Kapur’s entropy. This algorithm

		approved their efficacy compared with the others when solving the ISP of the medical image
3	Maitra, Chatterjee [47]	PSO improved by cooperative and comprehensive learning has been developed for tackling the ISP. Both cooperative and comprehensive learning used with PSO to alleviate the dimensionality curse and prevent the early convergence
4	Liu, Y., et al. [48]	The PSO has been modified using adaptive inertia and the adaptive population for tackling the ISP. Adaptive inertia is used to promote the convergence speed of PSO, while the adaptive population is used to prevent stuck into local optima.
5	Ghamisi et al. [49]	Fractional-order Darwinian PSO has been proposed for overcoming the image segmentation problem based on the Otsu function. The Fractional-derivative was used with PSO to dominate the convergence rate.
6	El Aziz [33]	WOA and MFA were proposed for tackling the ISP by maximizing otsu method, although just for threshold levels reaching 6
7	Chen [50]	In this paper, The Improved FFA (IFFA) has been proposed for solving ISP. IFFA was improved using the Cauchy mutation to avoid local minima and neighborhood strategy to enhance the convergence
8	Agrawal[36]	In this paper, CS has been proposed to extract the optimal threshold values of an image by maximizing the Tsallis entropy.
9	Bhandari[51]	In this paper, the satellite image was segmented using ABC based on maximizing a variety of objective functions. ABC was improved using a chaotic search to initialize the population at the outset and the differential evolution to enhance the exploitation capability.
10	Sanya[52]	The fuzzy entropy to change between the exploration and exploitation operators was used with The bacterial foraging algorithm (BFA) for getting to the optimal threshold values of an image.
11	Sathya[53]	In this paper, to accelerate the premature convergence of BFA when solving ISP, the best bacteria among all the chemotactic steps is moved to the subsequent generations.
12	Tang[53]	This paper integrated the PSO with BFA to provide the global search capability and promote the premature convergence towards the optimal threshold values
13	Abdel-Basset [54]	A novel equilibrium optimizer (EO) has been proposed for finding the optimal threshold values of an image by maximizing the Kapur's entropy.
14	Abdel-Basset [55]	A novel marine predators algorithm (IMPA) improved using the Ranking-based diversity reduction strategy has been suggested to segment the chest X-ray image
15	Chouksey[56]	In this paper, the antlion optimization (ALO) and the multiverse optimization (MVO) have been developed for tackling the ISP by maximizing the Kapur's entropy and Otsu method. After investigating the performance of ALO, and MVO, the author notified that MVO is better
16	Erik Cuevas[44]	In this paper, the locust search algorithm (LSA) was applied for solving the multi-level thresholding image segmentation under a new objective function in a gaussian mixture model.

All the algorithms listed in the literature were proposed for overcoming the ISP of a normal image and medical image of type X-Ray images, but no one of which is experimented on the X-ray images that are considered the most important thing to detect the infection with COVID-19. Currently, there are two ways to be blended for much better performance. First, the high ability of WOA can be used to explore a new region to find a better solution within the first half of iterations. Second, the high capacity of SMA can be used to balance between exploitation and exploration. Thus, authors are motivated to make a hybridization between them to propose a new model to combine those two capabilities for overcoming the ISP for COVID-19 X-ray images. Broadly speaking, the SMA is integrated with WOA to finding a better solution, where the WOA will be run within the first CI iteration to explore various regions within the search space. Afterward, the SMA will take the solutions obtained by WOA to exploit them or explore at the expense of the fitness of each solution as an attempt to use up this capability of SMA. Additionally,

SMA increases its exploration capability to escape out of the local minima by re-initializing the current solution randomly within the search space of the problem based on a certain probability. This hybrid approach is abbreviated as HSMA_WOA. SMA and HSMA_WOA are compared with several state-of-the-art algorithms under X-ray test images infected with COVID-19. After comparison, we saw that HSMA_WOA could outperform all the algorithms used to compare most of the test images used in our experiment.

3. Kapur's entropy

In this section, the mathematical model of Kapur's entropy method is shown. Kapur's entropy searches for the optimal threshold values by maximizing the variance between the segmented regions [20]. The mathematical model of this method is described as follows:

supposing that $[r_0, r_1, r_2, \dots, r_T]$ refers to the threshold values that subdivide the image into a different similar area, then the Kapur's entropy can be calculated as follows:

$$R(r_0, r_1, r_2, \dots, r_T) = R_0 + R_1 + R_2 + \dots + R_T \quad (1)$$

where:

$$R_0 = -\sum_{i=0}^{r_0-1} \frac{X_i}{W_0} * \ln \frac{X_i}{W_0}, X_i = \frac{N_i}{W}, W_0 = \sum_{i=0}^{r_0-1} X_i \quad (2)$$

$$R_1 = -\sum_{i=r_0}^{r_1-1} \frac{X_i}{W_1} * \ln \frac{X_i}{W_1}, X_i = \frac{N_i}{W}, W_1 = \sum_{i=r_0}^{r_1-1} X_i \quad (3)$$

$$R_2 = -\sum_{i=r_1}^{r_2-1} \frac{X_i}{W_2} * \ln \frac{X_i}{W_2}, X_i = \frac{N_i}{W}, W_2 = \sum_{i=r_1}^{r_2-1} X_i \quad (4)$$

$$R_T = -\sum_{i=r_T}^{L-1} \frac{X_i}{W_T} * \ln \frac{X_i}{W_T}, X_i = \frac{N_i}{W}, W_T = \sum_{i=r_T}^{L-1} X_i \quad (5)$$

$R_0, R_1, R_2, \dots, R_T$ refer to the entropies obtained by each threshold value, and N_i indicates the count of the pixels having a value I , the grey level. And $W_0, W_1, W_2, \dots, W_T$ refers to the percent of the pixels in each region to the pixels in the whole image. And T indicates the threshold levels.

In order to extract the optimal threshold values, the following equation is maximized:

$$F(r_0, r_1, r_2, \dots, r_T) = \max\{R(r_0, r_1, r_2, \dots, r_T)\} \quad (6)$$

The proposed algorithm will use Eq.6 as an objective function to get the optimal threshold values.

4. Standard whale optimization algorithm (WOA)

In WOA [57], the behaviors of the humpback whales are simulated to proposed new optimization algorithms for tackling the continuous optimization problems. These whales move surround the prey in a spiral shape and then move toward prey in a shrinking circle when attacking. This behavior is called bubble-new foraging. This hunting mechanism is mimicked within the WOA by a trade-off between a spiral model and a shrinking encircling prey with a probability of 50%, generating the new solution within the optimization process. The encircling mechanism is athletes described as follows:

$$\vec{S}(t+1) = \vec{S}^*(t) - \vec{A} \cdot \vec{D} \quad (7)$$

$$\vec{A} = 2\vec{a} \cdot \overline{rand} - \vec{a} \quad (8)$$

$$\vec{a} = 2 - 2 \frac{t}{t_{max}} \quad (9)$$

$$\vec{D} = |\vec{C} \cdot \vec{S}^*(t) - \vec{S}(t)| \quad (10)$$

$$\vec{C} = 2 \cdot \overline{rand} \quad (11)$$

where \vec{S} is a vector that expresses the current whale, t is the current generation, \vec{S}^* refers to the values of the best whale in the population, \vec{r} is a numerical vector generated randomly between 0 and 1. t_{max} refers to the maximum generations, and a is a parameter linearly decreased from 2 to 0 and is the distance control factor. The distance between the position of the victim and the whale is used where the helix-shaped movements simulated by a spiral model are done. The spiral model is mathematically modeled as:

$$\vec{S}(t+1) = \vec{S}^*(t) + \vec{D}^l \cdot e^{lb} \cdot \cos(2\pi l) \quad (12)$$

$$\vec{D}^l = |\vec{S}^*(t) - \vec{S}(t)| \quad (13)$$

where \vec{D}^l is the difference between the best-so-far solution and i^{th} solution, l is a number created randomly between $[-1, 1]$, the logarithmic spiral shape is described by b as a constant. The best-so-far solution may be a local minima problem, so focusing completely on it within the optimization process may waste the search process within any beneficial mentioned. Therefore, the whale search for another position may contain the prey within the search area by picking a random whale from the population to move the current whale toward finding a better solution. Specifically, if $\vec{A} < 1$, then the current whale is directed based on a whale picked randomly from the population. The mathematical model of this exploration phase is:

$$\vec{S}(t+1) = \vec{S}^*(t) - \vec{A} \cdot \vec{D} \quad (14)$$

$$\vec{D} = |\vec{C} \cdot \vec{S}_{rand}(t) - \vec{S}(t)| \quad (15)$$

where \vec{S}_{rand} is a position vector picked randomly from the population. Finally, the steps of the standard WOA are listed in Algorithm 1.

Algorithm 1 The standard WOA

1. Initilaization $S_i (i = 1, 2, 3, \dots, N)$
 2. Evaluate each \vec{S}_i using the fitness function
 3. Find the best s^*
 4. $t = 1$ // current iteration
 5. **while** ($t < t_{max}$)
 6. **for** each \vec{S}_i
 7. Update a, A, p, C , and l
 8. **if** ($p < 0.5$)
 9. **if** ($|A| < 1$)
 10. Update $\vec{S}_i(t+1)$ based on Eq. (7)
 11. **else**
 12. Update $\vec{S}_i(t+1)$ based on Eq. (14)
 13. **end if**
 14. **else**
 15. Update $\vec{S}_i(t+1)$ based on Eq. (12)
 16. **end if**
 17. **end for**
-

-
18. Check the fitness value of each updated \vec{S}_i
 19. Update the best \vec{S}^* with \vec{S}_i if better.
 20. $t++$
 21. **end while**
-

5. Slime mould algorithm (SMA).

Chen [56] has recently been proposed a new optimization algorithm inspired by the behaviors of the slime mould in obtaining the optimal path for connecting food. This algorithm was known as the slime mould algorithm (SMA). The mathematical model of the SMA based on Chen proposition [56] is described in the following.

In the first stage, when SMA searches for the food, it uses its odor in the air as a means of reaching the food. Based on the behavior of the slime mould, it is formulated as follows to simulate the contraction mode [58] :

$$\vec{S}(t+1) = \begin{cases} \vec{S}_b(t) + \vec{vb} * (\vec{W} * \vec{S}_A(t) - \vec{S}_B(t)), & r < p \\ \vec{vc} * \vec{S}(t), & r \geq p \end{cases} \quad (16)$$

\vec{vb} is randomly generated within $[a, -a]$ as:

$$\vec{vb} = [-a, a] \quad (17)$$

$$a = \text{arctanh}\left(-\left(\frac{t}{t_{max}}\right) + 1\right) \quad (18)$$

And \vec{vc} linearly decreases from 1 to 0, t indicates the iteration current, t_{max} indicates the maximum of iteration, \vec{S}_b is a vector that contains the location with the highest odor concentration found so far. $\vec{S}(t+1)$ indicates the next position taken by the current slime mould (SM). $\vec{S}(t)$ is the current position of the SM, and \vec{S}_A and \vec{S}_B are two vectors containing the location of two randomly selected individuals from the population. The variable r is a random number between 0 and 1. \vec{W} describes the slime mould weight and calculated as follows:

$$\vec{W}(\text{smellindex}(l)) = \begin{cases} 1 + r * \log\left(\frac{bF - S(i)}{bF - wF} + 1\right), & \text{condition} \\ 1 - r * \log\left(\frac{bF - S(i)}{bF - wF} + 1\right), & \text{other} \end{cases} \quad (19)$$

$$\text{smellindex} = \text{sort}(S) \quad (20)$$

where r is a random number created within the range of 0 and 1, bF is the best fitness value within the current iteration, while wF stands for the worst one, smellindex refers to the indices of the sorted fitness values, condition indicates $S(i)$ ranks of the first half of the population. In relative to parameter p in Eq.21 is modeled as follows:

$$p = \tanh(|f(i) - DF|) \quad (21)$$

where $i \in 1, 2, 3, \dots, n$, $f(i)$ is the fitness of the current \vec{X} , DF is the best fitness obtained so far.

In the second phase, the wrapped phase simulates the contraction mode in the venous structure of slime mould, which tunes their positions according to the quality of the food, when the food concentration is high, the weight of this region is bigger. Otherwise, the region's weight is turned to explore other regions, as shown in Eq.15. The SM needs to decide when to leave the current area to another one until finding a variety of food sources at the same time rather than the current better one. Generally, the mathematical model of updating the SM position could be re-modeled, as shown in Eq. 18 to simulate the methodology of the SM to find various food sources at the same time when foraging another area.

$$\vec{S}^*(t+1) = \begin{cases} rand * (UB - LB) + LB, rand < z \\ \vec{S}_b(t) + \vec{vb} * (\vec{W} * \vec{S}_A(t) - \vec{S}_B(t)), r < p \\ \vec{vc} * \vec{S}(t), r \geq p \end{cases} \quad (22)$$

where *rand* and *r* are two numbers generated randomly between 0 and 1, and *UB* and *LB* are the upper and lower bounds of the problem's search space. *z* is a probability used to determine if the SMA will search for another food source or search around the best current one. In relative to \vec{W} , \vec{vb} , and \vec{vc} , they are used to mimic the venous width variation. Finally, the steps of SMA are presented by Algorithm 2.

Algorithm 2 The Slime mould algorithm (SMA)

1. Initializations step
2. **While** ($t < t_{max}$)
3. Evaluate each S_i
4. Update the global best fitness GF , and global best position GP
5. Compute W using Eq.19
6. **for** each S_i
7. Update p , vb , and vc
8. Update S_i based on Eq.22
9. **end for**
10. $t++$
11. **end while**
12. Output: return GF , GP

6. The proposed work.

Within this part, our methodology for overcoming ISP for COVID-19 X-ray images will be illustrated in detail to show our plan for finding the threshold values that will help in extracting the region of interest within the infected images. Specifically, within this section, the following steps that contract the main structure of our proposition will be discussed: Initialization, SMA for ISP, hybrid SMA with WOA.

6.1. Initialization

As an inhabit of all the meta-heuristic algorithms, a set consists of N solutions has been proposed at the start. Each one has a number of dimensions distributed within 0 and 255 randomly using Eq.23.

$$\vec{S}_i = \vec{L}_{min} + \vec{r} * (\vec{L}_{max} - \vec{L}_{min}) \quad (23)$$

Where \vec{L}_{min} , and \vec{L}_{max} indicate the boundaries of the gray levels, \vec{r} is a random numerical vector in the range of $[0, 1]$, and \vec{S}_i indicates the i^{th} solution.

6.2. SMA for ISP

Last but not least, SMA is adapted for overcoming the ISP of the COVID-19 X-ray images by maximizing Kapur's entropy. This adaptation will help in extracting similar regions within images that may contain similar features of COVID-19. The main advantages of SMA include a high ability to balance between exploration and exploitation. When the distance between the fitness of the current individual is high, it will try to move toward it in an attempt to exploit it. Meanwhile, if the distance is small, then it will explore another food source to find a better solution. Finally, the steps of SMA for overcoming ISP are listed in Algorithm 3.

Algorithm 3 adapting SMA for ISP	
1.	Initializations step, $S_i, i = 0, 1, 2, 3, 4, \dots, N$
2.	While ($t < t_{max}$)
3.	Compute the fitness of each S_i using Eq.6.
4.	Update the global best fitness GF , and global best position GP
5.	Compute W using Eq.19
6.	for each S_i mould
7.	Update p , vb , and vc
8.	Update S_i using Eq.22
9.	end for
10.	$t++$
11.	end while
12.	Output: return GF, GP

6.3. Hybrid SMA_WOA (HSMA_WOA)

In this version, the SMA will be used with the WOA for tackling the ISP, where the SMA is used to pay attention to the best so-far regions obtained by the WOA. At the same time, the WOA is applied at the start of the optimization process until a predefined iteration CI is reached. CI is the end iteration where the WOA will stop and SMA starts. Specifically, WOA is applied at the outset to use up its exploration capability within the first half of the iteration for exploring the search space. After reaching the CI, the WOA will be stopped. SMA then starts to pay attention to searching for a better solution using the high-ability of SMA that will exploit around the best-so-far if the distance between the fitness value of the current solution and the best-so-far solution is higher than a specific value generated randomly. Otherwise, it will work on exploring another region searching for a better food source. In addition to disposing of the local minima using the SMA's exploration capability that re-initialized the solutions that were within a predefined probability randomly within the search space. This hybridization is aimed to exploit the exploration capability of the WOA at the start. The next step is to enhance the significant balancing capability of SMA and increase their ability to get out of local minima. Therefore, this can achieve full exploration capability when a number generated random SMA is less dependent on the z factor.

The main advantages of this model are as follows:

1. By using the high-ability of the WOA at the start of the optimization process, it can explore most of the regions within the search space to find a better solution.

2. After exploring the search space using the exploration capability of WOA, the SMA is used to exploit around the best-so-far solution if the distance between the fitness of the current one and the best-so-far fitness is higher than a threshold value generated randomly between 0 and 1. Otherwise, the current SM will try to explore another region for another best-so-far solution. Additionally, SMA used another capability to explore another region for a better solution. This capability is based on re-initializing randomly the current mould within the search space of the problem according to a certain probability.
3. This high-ability on exploring at the first half of the optimization process and adjusting that determines if the exploration or exploitation capability will be used within the second half of the optimization process help in proposing a model with high-ability on exploration, exploitation and avoiding dropping into local minima.
4. Having only two parameters, r and CI need to be updated accordingly.

The main drawbacks of this model are as follows:

1. Difficulties in picking the relevant value for CI can lead to using up the ability of this hybridization.
2. It still suffers from the probability of falling into local minima problem if the best-so-far solution obtained by WOA is local minima. The value of z of the SMA used to escape local minima is small, and increasing this value will enhance the probability of randomly re-initializing the current solution within the search space and, subsequently, the convergence toward the best solution significantly reduce.

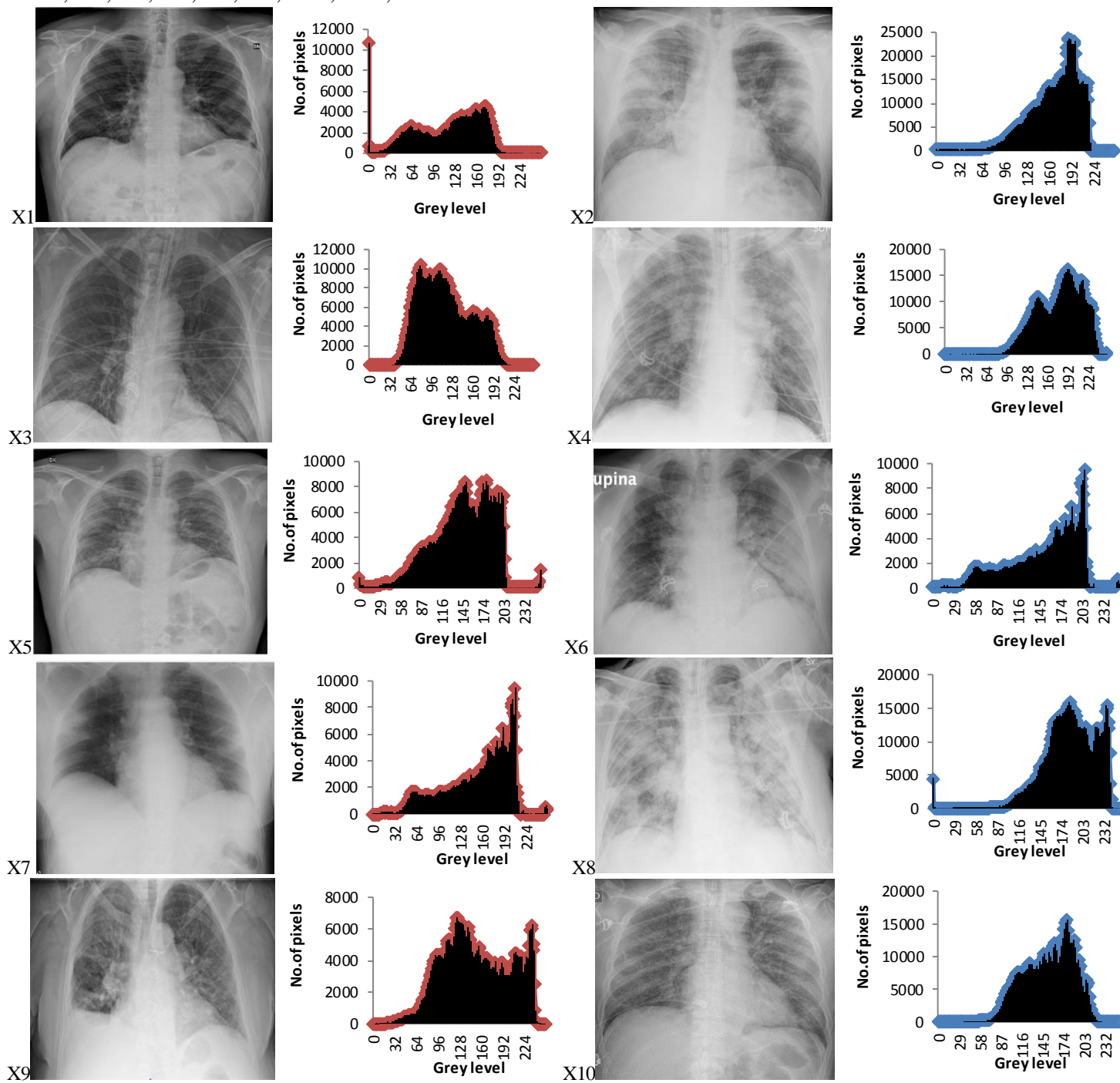
At the final, the final brief steps for the hybridization of both WOA and SMA are presented by Algorithm 4.

Algorithm 4 HSMA_WOA	
1.	Initializations step, $S_i, i = 0, 1, 2, 3, 4, \dots, N$
2.	While ($t < t_{max}$)
3.	If ($t < CI$)
4.	Apply the WOA shown in Algorithm 1
5.	Continue;
6.	end if
7.	Compute the fitness of each S_i using Eq.6
8.	Update the global best fitness GF , and global best position GP
9.	Compute W using Eq.19
10.	for each S_i mould
11.	Update p, vb , and vc
12.	Update S_i using Eq.22
13.	end for
14.	$t++$
15.	end while
16.	Output: return GF, GP

7. Results and discussion

In this section, extensive experiments have been conducted to validate the proposed algorithms' performance and compare their performance with some of the state-of-the-art algorithms when tackling the

ISP. Those experiments were performed on a set of chest X-ray COVID-19 images, namely X1, X2, X3, X4, X5, X6, X7, X8, X9, X10, X11, and X12.



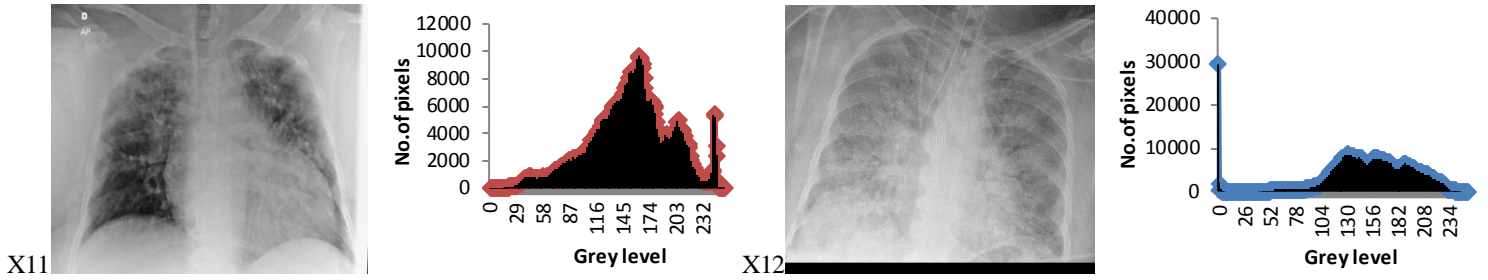


Fig. 1 the original COVID-19 images and their histograms

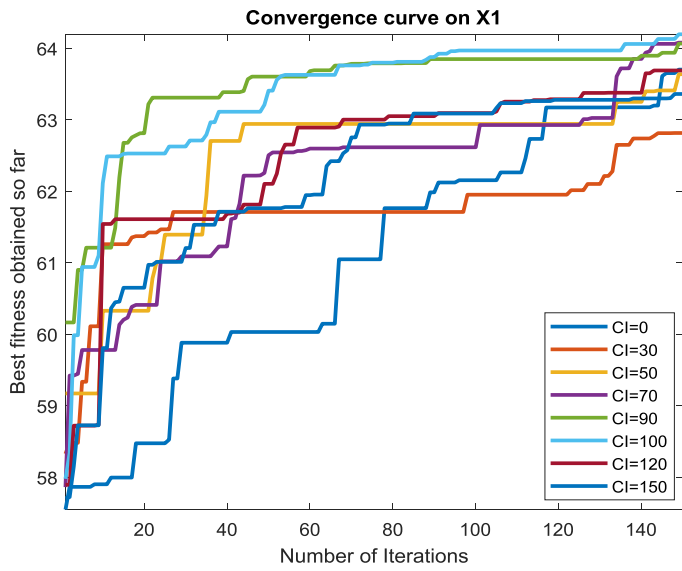
Additionally, a device equipped with 32-bit windows seven ultimate has been prepared for conducting our experiments. This device has the following capabilities:

- Core i3 processor with speed 2.20 GHz
- 1 GB of RAM

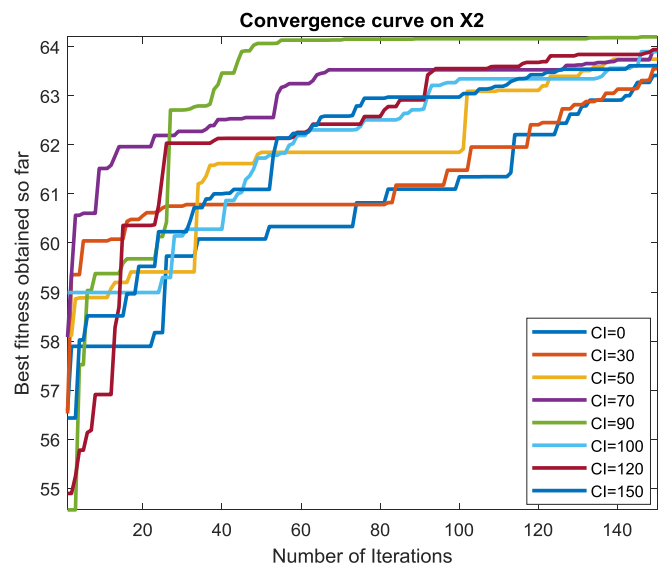
In order to check the efficacy of the proposed algorithm, it is compared with several well-known algorithms, such as Lshade [59], FFA [39], WOA [33], SSA [60], and HHA [38]. All those algorithms are further implemented using Java programming language. For the compared algorithms, the parameter values are the same as found in the original paper rather than the maximum iteration and population size that are set to 150, and 30 respectively, for a fair comparison. Additionally, all algorithms run 20 independently times to check the stability and consistency of the results obtained by each one.

Regarding our proposition, the CI parameter needs to be carefully picked for reaching the best performance for this approach, so several values for it, such as 0, 30, 50, 70, 90, 100, 120, and 150, are checked under test images X1, X2 and X3 to see the best value. And after running the algorithm under each CI value 20 independent runs and drawing the convergence curve of the best run for X1, X2 and X3 in Fig.2 (a), (b), and (c), respectively, we witness that the value 100 is the best for it on X1, and X3. While CI=90 is the best on X2 and its performance is converged with CI=100 on X3. So, the best two candidate values for CI under our experiments are 90 and 100.

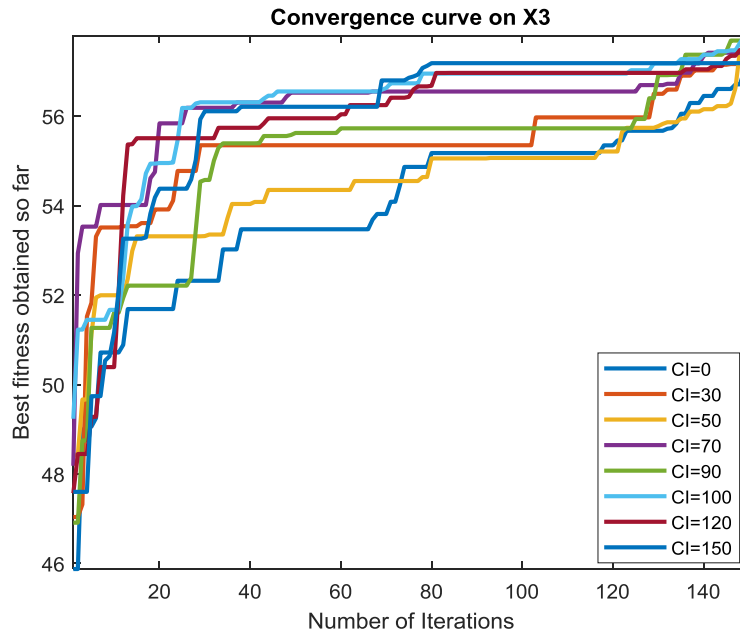
Regarding the r parameter, five values, such as 0.01, 0.02, 0.03, 0.04, and 0.04, are selected to test the performance of the proposed algorithm under them. After running the algorithm under each r value 20 independent runs, the best run for each value is pictured in Fig.2(d) and (e) for X1 and X2, respectively. According to those figures, $r=0.02$ is the best among the others, so it will be used for r within the next extensive experiments. Finally, Table 2 gives the parameter values of the proposed algorithm.



a. Convergence curve under different CI values on X1 with T=30.



b. Convergence curve under different CI values on X2 with T=30.



c. Convergence curve under different CI values on X3 with T=30.

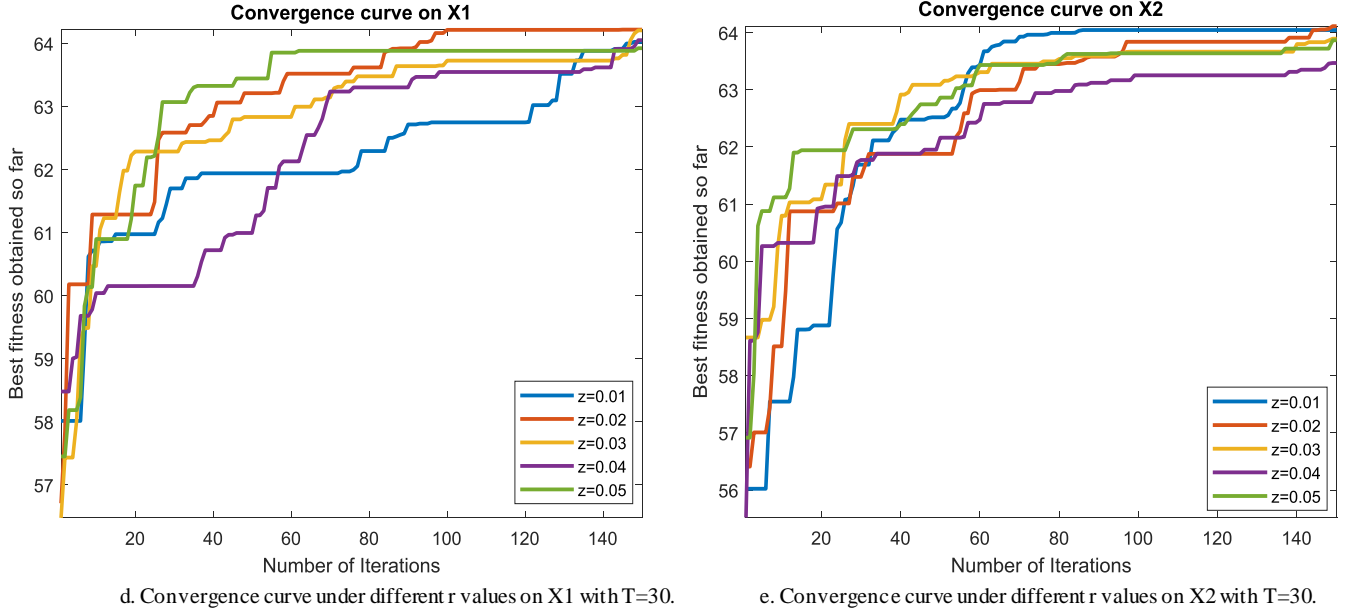


Fig.2 Adjustment of CI and z parameters

Table 2 Parameter setting for the proposed

Parameter	Value
Number of runs	20
Population size	30
The maximum number of iteration	150
Z	0.02
CI	100

The remainder of this section is listed as follows:

1. Section 7.1: Analyzes the Stability and CPU time.
2. Section 7.2: Discusses the quality of images using Fitness values.
3. Section 7.3: Discusses the quality of images using peak signal to noise ratio.
4. Section 7.4: Discusses the quality of images using a structured similarity index metric.
5. Section 7.5: exposes the outcomes of the universal quality image metric.
6. Section 7.6: Convergence rate among SMA, HSMA_WOA, and WOA.

7.1. Stability and CPU time analysis.

In this section, the time taken by each algorithm until finding the threshold levels is observed to see any algorithm could achieve the minimum of time. In addition, some algorithms produce spaced-out results in the different runs, so the stability of the obtained has to be calculated to see which algorithm could achieve converged results in all. This is known using the standard deviation (*Std*) calculated based on the following formula:

$$Std = \sqrt{\frac{1}{n-1} \sum_{i=1}^n (f_i - \bar{f})^2} \quad (24)$$

Where n indicates the number of times, each algorithm tried. f_i is the fitness value of the i^{th} run, and \bar{f} is the average of all the fitness values gotten. SD must be minimized to get to a better result.

Under Kapur's function, respectively, Fig. 3, and 4 show the average of SD and CPU time values obtained by each algorithm within 20 independent runs. As a result of inspecting those figures, HSMA_WOA could reach less SD and CPU time values, while Lshade, and HHA achieve the worst value for both Std and CPU time.

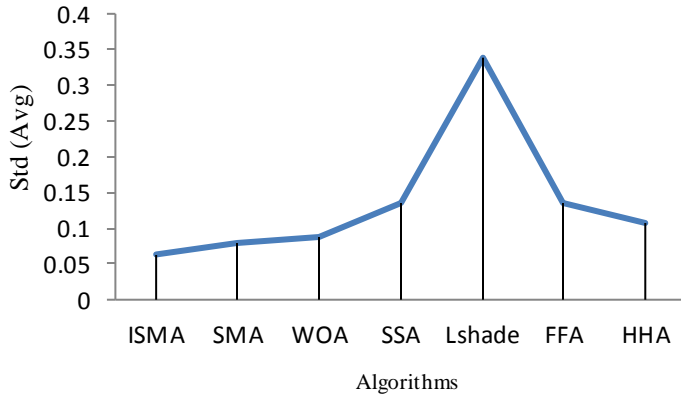


Fig. 3 the Std values obtained under Kapure's function

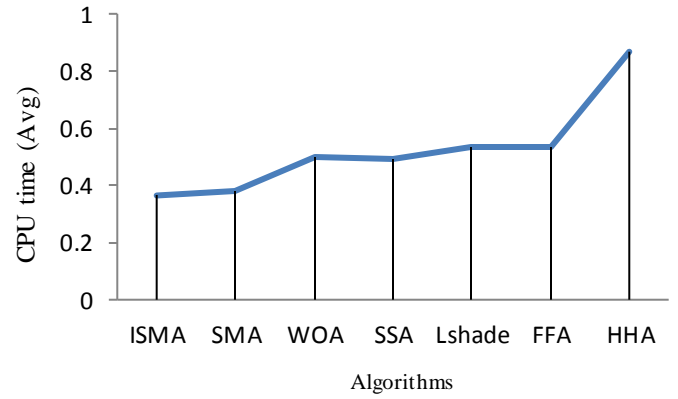


Fig. 4 Comparison of the CPU time values obtained under Kapur

7.2 Fitness values under Kapur.

Regarding the fitness values of Kapur's method, Table 3 shows the fitness values obtained by the compared algorithm and the proposed under this function. After calculating the average of the fitness values within 20 runs on each threshold level for each image, those values are recorded in Table 3 and displayed graphically in Fig.5. Based on this table, the proposed could outperform the others in most cases. This is confirmed based on Fig.5 that shows the superiority of the proposed algorithm with a value of 29.29 compared with the others with a difference of at least 0.0418.

Table 3: Fitness values of each algorithm under Kapur's entropy.

img	T	HSMA_WOA	SMA	FFA [39]	WOA [33]	SSA [60]	HHA [38]	LShade [59]	Img	HSMA_WOA	SMA	FFA [39]	WOA [33]	SSA [60]	HHA [38]	LShade [59]		
X1	2	12.2074	12.2074	12.2074	12.2068	12.2074	12.2074	12.1556	X7	12.2964	12.2967	12.2967	12.2964	12.2967	12.2967	12.2777		
	3	15.4120	15.4120	15.4120	15.4119	15.4120	15.4119	15.2913		15.5549	15.5548	15.5549	15.5548	15.5548	15.5548	15.5547	15.3888	
	4	18.3112	18.3112	18.3108	18.3102	18.3104	18.3108	18.0011		18.4683	18.4683	18.4681	18.4682	18.4682	18.4681	18.4680	18.1718	
	5	20.9774	20.9776	20.9758	20.9751	20.9760	20.9753	20.5394		21.1420	21.1417	21.1395	21.1418	21.1398	21.1410	21.1410	20.6861	
	6	23.4434	23.4440	23.4375	23.4412	23.4358	23.4416	22.8031		23.6338	23.6324	23.6265	23.6337	23.6297	23.6326	23.6326	22.9432	
	7	25.7537	25.7343	25.7294	25.7547	25.7436	25.7337	24.9663		25.9929	25.9718	25.9499	25.9919	25.9322	25.9826	25.9826	25.2158	
	8	27.9823	27.9577	27.9280	27.9621	27.9293	27.9527	26.9708		28.3005	28.2498	28.1752	28.2776	28.1857	28.2527	28.2527	27.2256	
	9	30.1637	30.1407	30.0533	30.1534	30.0713	30.1281	29.1068		30.4908	30.4411	30.3546	30.4587	30.3330	30.4322	30.4322	29.2097	
	10	32.2340	32.2322	32.0841	32.2147	32.1798	32.1957	30.8905		32.6062	32.5833	32.5143	32.5549	32.5056	32.5387	32.5387	31.1228	
	15	41.5906	41.5320	41.3379	41.5832	41.4564	41.4961	39.3727		42.3377	42.3673	41.8330	42.1271	41.8258	41.8732	41.8732	39.5835	
	20	50.1159	50.0046	49.7143	50.1298	49.9001	49.6968	46.7057		50.3917	50.4087	49.6449	50.1529	49.5730	49.7524	49.7524	46.6173	
	30	63.8093	63.7036	63.2656	63.8746	63.4349	62.7237	58.4513		63.8513	63.2789	62.8727	62.7227	62.5030	62.6031	62.6031	58.4957	
	X2	2	12.6324	12.6324	12.6324	12.6324	12.6324	12.6324		12.6044	X8	12.3441	12.3441	12.3441	12.3441	12.3441	12.3441	12.3095
		3	15.7263	15.7263	15.7263	15.7263	15.7263	15.6539		15.4573		15.4573	15.4573	15.4573	15.4573	15.4573	15.4573	15.3512
		4	18.7055	18.7054	18.7052	18.7055	18.7053	18.7054		18.4603		18.1902	18.1884	18.1867	18.1887	18.1945	18.1959	18.0256
5		21.4534	21.4532	21.4522	21.4533	21.4528	21.4531	21.0459	20.8900	20.8896		20.8809	20.8895	20.8880	20.8898	20.8898	20.6162	
6		24.0311	24.0238	24.0237	24.0295	24.0248	24.0304	23.4316	23.4203	23.4146		23.4043	23.4177	23.4019	23.4168	23.4168	23.0338	
7		26.4825	26.4711	26.4763	26.4821	26.4789	26.4805	25.5994	25.8917	25.8778		25.8747	25.8904	25.8771	25.8906	25.8906	25.3007	
8		28.8380	28.8289	28.7895	28.8381	28.7971	28.8337	27.7372	28.2040	28.1926		28.1680	28.1957	28.1705	28.1858	28.1858	27.4058	
9		31.0405	31.0292	31.0151	31.0395	31.0096	31.0283	29.5524	30.4411	30.4344		30.3963	30.4455	30.3813	30.4329	30.4329	29.6020	
10		33.1868	33.1659	33.1504	33.1946	33.1522	33.1614	31.5542	32.6168	32.5619		32.4833	32.5955	32.4729	32.5696	32.5696	31.5018	
15		42.6820	42.6037	42.5246	42.7080	42.5106	42.5746	38.9055	42.7217	42.5800		42.4650	42.6246	42.5328	42.5093	42.5093	40.8442	
20		50.7079	50.5412	50.4158	50.7806	50.2943	50.3530	45.7687	51.5077	51.3147		51.0380	51.2673	51.0484	51.0233	51.0233	48.3724	
30		63.8566	63.3631	63.0311	63.8308	63.0813	62.6600	56.8894	65.7863	65.4368		65.1388	65.3790	65.0701	64.6126	64.6126	60.6688	

X3	2	11.7581	11.7581	11.7581	11.7581	11.7581	11.7581	11.7534	X9	12.6276	12.6276	12.6276	12.6276	12.6276	12.6276	12.6022
	3	14.5988	14.5988	14.5988	14.5988	14.5988	14.5988	14.4816		15.8423	15.8423	15.8423	15.8423	15.8423	15.8423	15.7972
	4	17.1833	17.1832	17.1832	17.1832	17.1832	17.1833	16.9445		18.7937	18.7936	18.7936	18.7936	18.7936	18.7935	18.6185
	5	19.6124	19.6116	19.6108	19.6124	19.6109	19.6125	19.1511		21.5610	21.5605	21.5613	21.5602	21.5585	21.5634	21.3423
	6	21.9391	21.9349	21.9307	21.9388	21.9325	21.9388	21.0710		24.2487	24.2489	24.2449	24.2489	24.2438	24.2466	23.8325
	7	24.1795	24.1732	24.1435	24.1743	24.1512	24.1742	22.8515		26.7337	26.7297	26.7176	26.7325	26.7149	26.7305	26.1619
	8	26.2990	26.2891	26.2626	26.2988	26.2664	26.2935	24.6100		29.1067	29.1013	29.0893	29.1069	29.0719	29.1027	28.4645
	9	28.3243	28.3033	28.2610	28.3266	28.2817	28.3108	26.3513		31.4107	31.3829	31.3743	31.4094	31.3314	31.3819	30.3883
	10	30.2695	30.2522	30.1717	30.2758	30.1624	30.2327	27.9424		33.6113	33.5793	33.5479	33.5034	33.5391	33.5901	32.4441
	15	38.7253	38.7204	38.4560	38.6548	38.4627	38.5182	34.0568		43.6111	43.4979	43.3693	43.4066	43.3396	43.3413	41.2879
20	45.7534	45.8173	45.1861	45.3783	45.2480	45.2328	39.6107		52.1459	52.1104	51.6784	51.7949	51.6493	51.4513	48.8682	
30	56.8804	57.0820	55.9473	55.9056	56.1606	56.0479	48.6062		66.1320	65.9175	65.2294	65.6912	65.7141	65.1745	61.3303	
X4	2	11.5969	11.5969	11.5969	11.5922	11.5969	11.5969	11.5018	X10	11.4659	11.4659	11.4659	11.4659	11.4659	11.4658	11.4416
	3	14.6869	14.6869	14.6869	14.6869	14.6869	14.6865	14.3767		14.4734	14.4734	14.4734	14.4734	14.4734	14.3120	
	4	17.5072	17.5072	17.5057	17.5072	17.5000	17.5021	17.0861		17.1998	17.1997	17.1993	17.1991	17.1994	17.1994	16.9438
	5	20.1209	20.1205	20.1129	20.1199	20.1137	20.1110	19.3430		19.7327	19.7314	19.7288	19.7322	19.7272	19.7314	19.1657
	6	22.5707	22.5680	22.5443	22.5601	22.5491	22.5594	21.6035		22.1103	22.1136	22.1041	22.1126	22.0954	22.1114	21.2619
	7	24.8598	24.8493	24.7909	24.8597	24.7693	24.8236	23.5827		24.3413	24.3347	24.3276	24.3110	24.3121	24.3337	23.2309
	8	27.0702	27.0339	26.9016	27.0394	26.8738	26.9829	25.4259		26.5355	26.5175	26.5121	26.5258	26.5101	26.5241	25.0055
	9	29.2080	29.2076	28.9102	29.1391	28.9810	29.1070	27.2155		28.6495	28.6020	28.5441	28.6429	28.5219	28.5987	26.8410
	10	31.2598	31.1961	30.9021	31.1877	30.8910	31.1434	29.0150		30.6022	30.5700	30.4296	30.5823	30.4392	30.5532	28.1181
	15	40.3413	40.3433	39.5598	40.1708	39.3364	40.0304	36.4513		39.3277	39.2510	38.8889	39.2983	38.9420	39.0566	34.8619
20	47.9266	47.8417	46.5941	47.6547	46.6598	47.2432	42.4565		46.6662	46.5212	46.0319	46.6636	46.0741	46.2364	40.8092	
30	60.0793	59.6827	58.0592	59.6088	58.2804	59.1605	52.8618		57.9616	57.9755	57.1485	57.6431	56.8034	57.3010	50.4033	
X5	2	12.2716	12.2716	12.2716	12.2716	12.2716	12.2716	12.2343	X11	12.5867	12.5867	12.5867	12.5867	12.5867	12.5867	12.5640
	3	15.1753	15.1753	15.1753	15.1753	15.1753	15.1753	15.0662		15.8311	15.8311	15.8311	15.8310	15.8311	15.7465	
	4	17.9995	17.9995	17.9993	17.9995	17.9993	17.9991	17.7654		18.7378	18.7377	18.7376	18.7378	18.7375	18.7376	18.6008
	5	20.8227	20.8232	20.7797	20.8005	20.7691	20.8018	20.2735		21.4981	21.4977	21.4958	21.4977	21.4952	21.4969	21.2420
	6	23.3704	23.3589	23.3467	23.3463	23.3381	23.3406	22.6542		24.0897	24.0837	24.0810	24.0833	24.0753	24.0854	23.6556
	7	25.8073	25.8326	25.7707	25.7956	25.8197	25.7531	24.8665		26.5695	26.5703	26.5640	26.5760	26.5627	26.5638	26.0417
	8	28.1356	28.1180	28.0283	28.1002	28.0606	28.0664	26.9687		28.9554	28.9516	28.9416	28.9590	28.9469	28.9529	28.1990
	9	30.2882	30.2694	30.2412	30.2119	30.2515	30.1984	29.1365		31.2528	31.2362	31.1760	31.2486	31.1696	31.2182	30.4522
	10	32.5805	32.5036	32.4395	32.3911	32.4113	32.3871	31.1720		33.4313	33.4086	33.3633	33.4224	33.3296	33.4041	32.2970
	15	42.5845	42.5995	42.2694	42.2985	42.3155	42.2362	40.3625		43.2185	43.1243	43.0157	43.1955	43.0276	43.0623	41.0752
20	51.2666	51.2620	50.6443	50.8380	50.7128	50.6155	47.9260		51.9702	51.7279	51.4212	51.7075	51.3078	51.4473	48.6555	
30	65.4349	65.0206	64.2166	64.8382	64.3390	64.2387	60.5143		65.8829	65.4744	64.8427	65.3291	64.8827	64.5217	61.0966	
X6	2	12.3680	12.3680	12.3680	12.3680	12.3680	12.3680	12.3459	X12	11.5270	11.5270	11.5270	11.5270	11.5270	11.5270	11.5051
	3	15.5171	15.5171	15.5171	15.5171	15.5170	15.5170	15.4254		14.3421	14.3421	14.3421	14.3421	14.3421	14.3421	14.1520
	4	18.3767	18.3767	18.3763	18.3766	18.3766	18.3766	18.1390		16.9039	16.9038	16.9039	16.9039	16.9038	16.9038	16.4324
	5	21.0192	21.0135	21.0170	21.0150	21.0207	20.6942		19.2474	19.2462	19.2425	19.2474	19.2436	19.2467	18.5003	
	6	23.5388	23.5188	23.5184	23.5308	23.5222	23.5305	22.9603		21.4496	21.4303	21.3734	21.4494	21.3800	21.4478	20.6131
	7	26.2273	26.0760	26.0680	26.1715	26.0603	26.1610	25.3283		23.4149	23.4171	23.3540	23.4218	23.4021	23.4578	22.6905
	8	28.7099	28.6659	28.6314	28.6177	28.5135	28.6417	27.6532		25.5494	25.5592	25.5187	25.5551	25.5211	25.5676	24.7982
	9	31.1027	31.0934	30.8702	31.0039	30.9502	30.9094	29.9045		27.7060	27.7039	27.6170	27.7009	27.6496	27.6898	26.6235
	10	33.3305	33.3115	33.2345	33.2451	33.1824	33.0647	31.8420		29.7960	29.7688	29.6837	29.7730	29.6457	29.7596	28.5756
	15	43.2567	43.2632	43.0468	42.9601	42.8639	42.8860	41.0070		39.2299	39.2056	38.6952	39.0824	38.7402	38.8831	36.3898
20	51.8206	51.9327	51.5385	51.5309	51.4507	51.2959	48.2590		47.0948	46.9360	46.4421	46.9399	46.4491	46.6039	42.7844	
30	66.0900	65.7362	64.7226	65.4600	64.9066	65.0200	61.3966		59.7040	59.4203	58.0159	59.4729	58.1772	58.5367	53.0049	

Bold value expresses the best outcome.

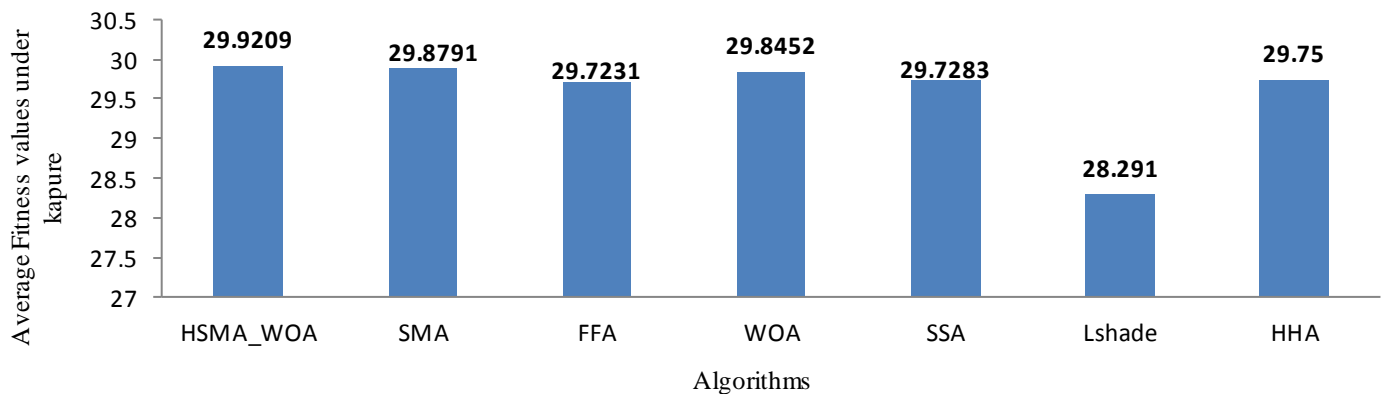


Fig. 5 average fitness values obtained under Kapur's method

7.3 Peak signal to noise ratio (PSNR)

In this section, another metric called PSNR has been used to measure the segmented image's quality compared with the original image. PSNR determines the ratio between the square of the maximum grey level, 255^2 , and the mean square error (MSE) between the original and separated one and it is calculated using as follows:

$$PSNR = 10 \log_{10} \left(\frac{255^2}{MSE} \right) \quad (25)$$

And MSE is calculated as shown in the following equation:

$$MSE = \frac{\sum_{i=1}^M \sum_{j=1}^N |A(i,j) - S(i,j)|}{M \times N} \quad (26)$$

Where $A(i, j)$ is the grey level of the segmented image and $S(i, j)$ is the grey level of the row i^{th} and column j^{th} in the original image matrix. M , and N are the number of columns and rows within the image. PSNR must be maximized to get to better quality.

Based on the segmented images under Kapure's function, the average PSNR value within 20 runs is calculated and introduced in Table 4. By observing this table, it is obvious that HSMA_WOA could be superior in 59 cases and equal in 14 out of 144, while SMA could be the best for 26 cases and equal in 14 out of 144. Generally, the proposed algorithms could be superior and equal in 104 out of 144. As a result, both SMA and HSMA_WOA could reach better-segmented images in all the superior cases compared with the other algorithms. In order to illustrate the results in Table 4 graphically, Fig. 6 is given to show the average of the PSNR values obtained by each algorithm. Based on this figure, the proposed algorithms: SMA, HSMA_WOA is considered superior compared with the others and HSMA_WOA is superior in comparison with SMA.

Table 4: PSNR values under Kapur's entropy.

img	T	HSMA_WOA	SMA	FFA [39]	WOA [33]	SSA [60]	HHH [38]	LShade [59]	Img	HSMA_WOA	SMA	FFA [39]	WOA [33]	SSA [60]	HHH [38]	LShade [59]
X1	2	13.1162	13.1162	13.1143	13.1134	13.1162	13.1162	12.8150	X7	15.2050	15.3933	15.3933	15.2050	15.3933	15.3933	15.1889
	3	16.4252	16.4252	16.4272	16.4224	16.4260	16.4342	16.0049		17.2119	17.2119	17.2103	17.2126	17.2103	17.2138	16.6914
	4	18.9556	18.9487	18.9706	18.9472	18.9729	18.9282	18.0015		19.4480	19.4630	19.4441	19.4513	19.4407	19.4623	18.5221
	5	21.2097	21.2093	21.3252	21.2233	21.3038	21.2017	19.5347		21.4352	21.4649	21.3603	21.4409	21.3665	21.4431	20.4637
	6	22.8398	22.8121	22.9398	22.8181	22.9310	22.7924	20.3662		22.8084	22.7867	22.6449	22.8054	22.6897	22.7897	20.5910
	7	24.1734	23.8189	23.9626	24.2318	24.1870	23.9846	21.6186		23.1957	23.7250	23.3627	23.0896	23.3614	23.2624	21.9508
	8	24.2804	24.7267	25.0769	24.4745	25.0152	24.3947	22.4469		23.8709	23.9958	23.7704	23.9287	23.9326	23.7384	22.3479
	9	25.3263	25.2232	25.9481	25.2295	25.8470	25.0828	23.3580		24.5680	24.3410	24.2142	24.5100	24.3554	24.5018	22.9391
	10	25.9865	26.1360	26.8390	26.0330	26.5743	25.8618	24.3433		25.1472	25.0194	24.5543	24.9923	24.5985	24.9951	23.0372
	15	29.4277	29.4927	29.8138	29.4908	29.8449	29.2103	26.5681		27.1336	27.1160	26.4416	27.1190	26.4248	26.4378	25.0565
20	31.6407	31.5051	31.8526	31.5302	32.0161	30.8344	29.0766	28.3797	28.3409	27.8586	28.2522	27.3527	27.6881	26.5497		
30	34.2147	34.7117	34.4426	34.2688	34.8958	33.4774	31.6066	29.5656	29.3375	29.1227	29.2851	28.9762	29.1881	28.4078		
X2	2	15.4339	15.4339	15.4339	15.4339	15.4339	15.4339	15.0664	X8	15.0584	15.0584	15.0584	15.0581	15.0584	15.0584	15.0231
	3	19.0614	19.0614	19.0598	19.0614	19.0598	19.0593	17.5684		18.5399	18.5397	18.5300	18.5398	18.5397	18.5384	18.3247
	4	19.5687	19.5676	19.5460	19.5845	19.5473	19.5785	19.0799		20.4752	20.4396	20.2559	20.3902	20.3021	20.3089	19.3735
	5	21.8944	21.9055	21.8064	21.9103	21.8351	21.8833	19.9896		21.7622	21.7326	21.4727	21.6882	21.3617	21.7624	20.7030
	6	23.3280	23.2037	23.1561	23.3193	23.1632	23.3404	21.1292		23.2417	23.0551	22.7673	23.1817	22.6722	23.1439	21.3987
	7	23.6048	23.7391	23.4373	23.6147	23.4716	23.6404	22.3326		23.8725	23.7568	23.6656	23.8724	23.7051	23.8228	22.1885
	8	25.2772	25.2649	24.7597	25.2939	24.8453	25.2088	22.7135		25.1533	25.1050	24.3448	24.9353	24.4041	24.8915	23.3818
	9	26.1459	26.0982	25.7633	26.2206	25.7351	26.0065	24.1776		26.0072	25.8164	25.1265	25.8631	25.1310	25.9092	24.3065
	10	26.8214	26.7884	26.3162	26.6867	26.3212	26.5252	24.6270		27.0580	26.6239	25.7109	26.8672	25.5503	26.6832	23.3187
	15	30.2230	30.2786	29.0026	30.3224	28.8439	29.7970	26.6702		28.4823	28.6101	27.4389	28.2749	27.9789	28.5384	26.9208
20	32.5178	32.2824	31.1105	32.6471	30.7657	31.6089	29.3500	31.0909	30.2209	29.5583	30.8247	29.2329	30.0101	28.1920		
30	35.6553	35.7611	33.5503	35.7363	33.8251	34.0759	31.9949	34.4386	33.9666	32.9237	34.4272	32.7464	33.1187	31.0745		
X3	2	13.5597	13.5597	13.5597	13.5597	13.5597	13.5597	13.5856	X9	13.9264	13.9264	13.9264	13.9264	13.9264	13.9264	13.9408
	3	15.4668	15.4608	15.4653	15.4668	15.4659	15.4668	15.8627		17.4209	17.4217	17.4209	17.4209	17.4200	17.4217	17.0266
	4	18.6812	18.6322	18.7060	18.6334	18.7064	18.6933	17.7343		19.7395	19.7373	19.7204	19.7387	19.7242	19.7436	18.6316
	5	20.5014	20.5286	20.9156	20.4033	20.8693	20.3339	18.6695		20.6141	20.6085	20.4564	20.5715	20.5183	20.5629	20.1364

	6	23.7724	23.5477	23.9135	23.7670	23.7958	23.7620	20.6607	22.2588	22.2602	22.2333	22.2654	22.2294	22.2429	21.0136	
	7	24.5192	24.4967	25.1493	24.5074	25.0146	24.4681	21.0312	23.6050	23.5830	23.3621	23.5882	23.3540	23.5769	22.2219	
	8	26.3355	25.9230	26.5196	26.2487	26.6897	26.1332	22.3935	24.4299	24.5225	24.2443	24.4996	24.1444	24.5016	22.8170	
	9	27.5838	27.2210	27.7576	27.5861	27.8061	27.5820	22.8420	25.2991	25.2872	25.0545	25.2862	24.9055	25.1897	23.3581	
	10	28.3308	28.2626	28.6363	28.2831	28.7330	28.2442	24.4468	26.1767	26.2434	25.8457	26.1998	25.8211	26.1591	23.7645	
	15	30.9231	31.3151	31.9472	30.5238	31.9835	30.8741	27.0095	29.0098	29.2177	28.8906	28.6140	28.6985	28.2695	26.2449	
	20	32.7470	33.3867	34.4622	32.3973	34.4528	32.4652	28.4250	31.4450	31.3282	30.6876	30.8601	30.6150	30.0195	28.5902	
	30	36.0843	36.9800	37.9711	35.5183	37.9570	35.8354	31.7538	34.7220	34.5881	33.3637	34.1399	33.7642	33.4018	31.5622	
X4	2	14.0817	14.0817	14.0817	14.1187	14.0817	14.0817	13.9607	X10	16.0138	16.0138	16.0138	16.0219	16.0138	16.0299	15.4414
	3	18.3927	18.3927	18.3927	18.3927	18.3927	18.3874	16.5780		19.4769	19.4769	19.4769	19.4801	19.4774	19.4774	18.4177
	4	20.8446	20.8528	20.8181	20.8524	20.7754	20.8269	18.6470		21.6089	21.6270	21.6471	21.6303	21.6809	21.6223	20.2690
	5	22.7884	22.7420	22.4952	22.7890	22.5426	22.7888	20.7013		23.5025	23.4975	23.4472	23.5018	23.4589	23.4938	20.9350
	6	24.3006	24.3038	24.0282	24.2793	24.0370	24.2615	21.2844		24.9480	24.9837	24.7865	25.0199	24.7514	24.9710	22.1587
	7	25.3571	25.4504	25.2328	25.4069	25.0215	25.1716	21.9359		25.8710	25.9455	25.5210	25.8056	25.3843	25.8204	22.9135
	8	26.0496	26.1674	25.8153	26.0798	25.6611	26.0980	22.6437		26.5926	26.7707	26.4238	26.5759	26.5108	26.4779	23.9432
	9	26.6098	26.5313	26.1939	26.1744	26.4447	26.6716	23.5580		27.7314	27.8226	27.5119	27.7398	27.3700	27.5431	24.5070
	10	27.3563	27.2461	26.8866	27.3559	26.8032	27.2050	24.3201		28.8519	28.7088	28.0721	28.8094	28.0597	28.5790	25.1122
	15	30.2457	29.8135	29.1392	30.2096	29.0109	30.1001	26.9848		31.6919	31.5349	31.0770	31.6099	31.2207	30.8728	26.8402
	20	32.2000	31.5708	30.9785	31.9510	30.2745	31.4728	28.1634		34.3762	33.6492	33.3989	34.0633	33.4870	33.1391	29.2939
	30	34.2907	33.3357	32.9391	33.8974	32.9951	33.6508	30.8160		36.6847	36.4906	36.1726	36.2996	35.5768	35.7522	32.5480
X5	2	16.8558	16.8558	16.8558	16.8558	16.8558	16.8558	16.5945	X11	14.2717	14.2717	14.2717	14.2717	14.2717	14.2717	14.2243
	3	19.9997	19.9997	19.9966	19.9987	19.9967	19.9975	18.5084		17.2552	17.2552	17.2540	17.2551	17.2540	17.2551	17.1190
	4	20.4189	20.3982	20.3662	20.4464	20.3874	20.4801	18.9831		19.9315	19.9244	19.9145	19.9315	19.9040	19.9273	19.1704
	5	20.6283	20.6116	20.7390	20.6807	20.8800	20.4794	20.1040		20.9527	20.9345	20.8917	20.9406	20.8786	20.9346	20.0765
	6	22.5190	22.2922	22.4222	22.4383	22.2021	22.3436	21.1247		22.2043	22.1748	22.0959	22.1603	22.0270	22.2015	20.9618
	7	23.4453	23.2175	22.9219	23.2131	22.8777	23.1368	21.8744		23.2544	23.2099	23.0703	23.2271	23.0977	23.2535	22.1135
	8	24.6961	24.5548	23.7161	24.6919	24.0570	24.2918	22.3592		24.2597	24.3125	24.0775	24.2580	24.1121	24.2203	22.7172
	9	25.2118	25.2193	24.3273	25.3126	24.2135	24.8847	22.8288		25.2773	25.2904	24.8579	25.2501	24.8420	25.0545	23.6391
	10	24.9566	25.0411	24.3275	24.8350	24.4260	24.9272	23.8191		26.1130	26.1173	25.7950	26.0308	25.6674	25.9849	24.1108
	15	27.5008	27.7911	27.1203	27.2337	26.8370	26.9085	25.6230		28.7869	28.7463	28.2373	28.6988	28.4623	28.5285	26.3509
	20	29.1286	29.1651	29.0824	28.6639	29.0095	28.4533	27.2341		30.8302	31.4031	30.6196	30.3909	30.5756	30.2222	28.2633
	30	30.7165	30.6026	30.5441	30.2876	30.7036	30.0646	29.4905		33.5412	33.3217	32.9252	32.9138	32.9945	32.0790	30.4614
X6	2	14.5488	14.5488	14.5488	14.5488	14.5488	14.5488	14.5558	X12	11.7366	11.7366	11.7366	11.7366	11.7366	11.7366	12.4388
	3	17.8770	17.8770	17.8753	17.8770	17.8671	17.8702	17.5791		14.7809	14.7809	14.7815	14.7797	14.7809	14.7782	11.1844
	4	19.8781	19.8781	19.8623	19.8749	19.8699	19.8702	18.9017		17.1519	17.0353	17.1667	17.1374	17.1667	17.1084	17.1003
	5	21.2166	21.2187	21.0808	21.1654	21.1375	21.2583	19.5376		18.0776	18.1041	18.4005	18.0776	18.3146	18.0667	18.0707
	6	21.5448	21.9494	21.8046	21.4509	21.5674	21.7895	20.0646		19.4659	19.6111	20.7148	19.4475	20.6380	19.4496	19.4717
	7	21.2614	21.9631	21.7077	21.1139	21.6558	20.9267	19.9842		24.1208	23.2142	24.0832	23.4850	23.8491	22.3931	22.3033
	8	22.1957	22.2642	21.7215	21.9257	22.1219	21.7240	21.3627		24.6843	25.7926	25.9087	25.6349	25.9052	25.8755	23.6704
	9	22.8453	22.7665	22.4835	22.6769	22.5525	22.5510	21.4795		26.8606	26.6221	26.6835	26.8531	26.7703	26.7230	24.2734
	10	23.6546	23.5141	23.2509	23.4438	22.8786	22.9563	22.0010		27.5479	27.5171	27.5659	27.7848	27.3789	27.8282	24.9804
	15	25.1382	25.1011	24.8791	24.9874	24.3782	24.7988	23.9355		30.6922	30.5015	30.4197	30.4398	30.6144	29.7160	26.9165
	20	25.9393	25.9809	25.6561	25.7365	25.6036	25.5312	24.9332		33.0374	33.0790	32.8630	32.9186	32.8577	32.3296	29.6352
	30	26.6336	26.6257	26.3605	26.5272	26.4522	26.3838	25.9521		36.5517	36.0368	35.5624	36.0258	36.1598	34.9519	31.0913

The bold value indicates the best value.

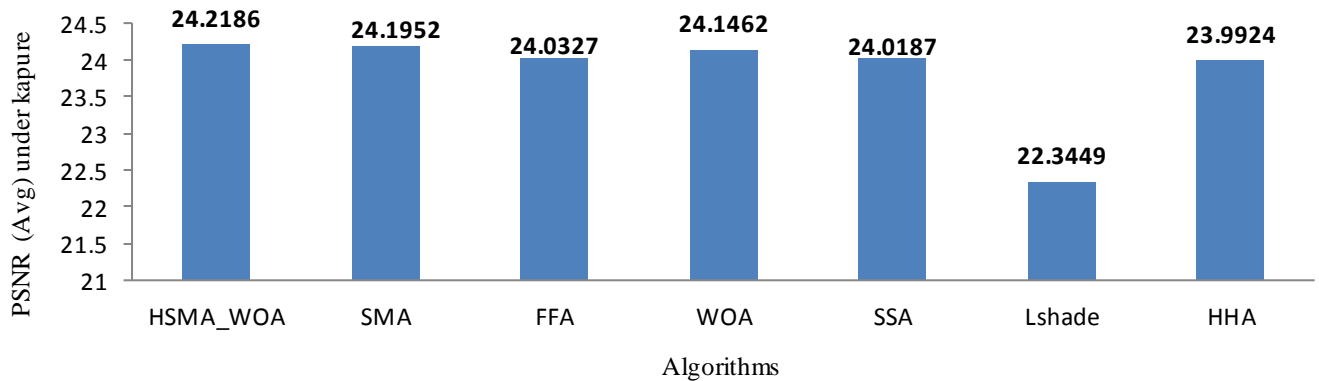


Fig.6 Average PSNR values under Kapure's entropy

7.4. Structured similarity index metric (SSIM)

Unfortunately, PSNR calculates only the ratio of the error between the segmented and the source image without taking into consideration the structure of the image. Therefore, SSIM [61] is proposed to measure the similarity, contrast distortion and brightness between the original and the segmented one using the following formula:

$$SSIM(O, S) = \frac{(2\mu_o\mu_s+a)(2\sigma_{os}+b)}{(\mu_o^2+\mu_s^2+a)(\sigma_o^2+\sigma_s^2+b)} \quad (27)$$

Where μ_o is the average intensities of the original image, while μ_s indicates the average intensities of the segmented image. σ_o, σ_s are the SD of the original and segmented images, respectively. σ_{os} are the covariance between the two images. And a, b is equal to 0.001 and 0.003, respectively. SSIM must also be maximized to get better results.

In order to inspect the results under using Kapur's entropy as a fitness function, the average SSIM values obtained within 20 runs under Kapur's are calculated and given in Table 5. This table shows that HSMA_WOA could get to the best in 57 cases and equal in 24 while its performance on the other cases is converged with the other algorithms. Meanwhile, SMA could outperform in 24 and equal in 22. Fig.7 shows the superiority of HSMA_WOA in comparison with SMA that is superior to the others.

Table 5: SSIM values under Kapure method.

img	T	HSMA_WOA	SMA	FFA [39]	WOA [33]	SSA [60]	HHA [38]	LShade [59]	Img	HSMA_WOA	SMA	FFA [39]	WOA [33]	SSA [60]	HHA [38]	LShade [59]			
XI	2	0.7439	0.7439	0.7439	0.7441	0.7439	0.7439	0.7250	X7	0.8638	0.8727	0.8727	0.8638	0.8727	0.8727	0.8637			
	3	0.8745	0.8745	0.8746	0.8746	0.8746	0.8748	0.8577		0.9038	0.9038	0.9036	0.9038	0.9036	0.9036	0.9036	0.8833		
	4	0.9243	0.9246	0.9248	0.9243	0.9246	0.9240	0.8993		0.9368	0.9370	0.9367	0.9368	0.9367	0.9370	0.9367	0.9370	0.9114	
	5	0.9524	0.9524	0.9537	0.9525	0.9535	0.9523	0.9271		0.9576	0.9578	0.9570	0.9577	0.9571	0.9577	0.9577	0.9427	0.9427	
	6	0.9654	0.9651	0.9669	0.9653	0.9667	0.9650	0.9364		0.9659	0.9658	0.9650	0.9660	0.9652	0.9657	0.9657	0.9387	0.9387	
	7	0.9741	0.9715	0.9730	0.9744	0.9714	0.9727	0.9498		0.9688	0.9706	0.9686	0.9685	0.9680	0.9689	0.9689	0.9559	0.9559	
	8	0.9746	0.9763	0.9782	0.9751	0.9781	0.9747	0.9570		0.9722	0.9721	0.9701	0.9723	0.9709	0.9710	0.9710	0.9571	0.9571	
	9	0.9791	0.9782	0.9818	0.9786	0.9815	0.9778	0.9658		0.9745	0.9733	0.9715	0.9744	0.9722	0.9740	0.9740	0.9598	0.9598	
	10	0.9816	0.9822	0.9849	0.9818	0.9840	0.9808	0.9720		0.9763	0.9759	0.9733	0.9758	0.9733	0.9755	0.9755	0.9607	0.9607	
	15	0.9910	0.9912	0.9916	0.9912	0.9918	0.9904	0.9825		0.9812	0.9811	0.9785	0.9812	0.9781	0.9785	0.9785	0.9712	0.9712	
	20	0.9939	0.9937	0.9940	0.9938	0.9943	0.9926	0.9893		0.9833	0.9833	0.9820	0.9829	0.9806	0.9814	0.9814	0.9776	0.9776	
	30	0.9956	0.9959	0.9957	0.9956	0.9960	0.9949	0.9930		0.9854	0.9848	0.9841	0.9848	0.9838	0.9845	0.9845	0.9828	0.9828	
	X2	2	0.8255	0.8255	0.8255	0.8255	0.8255	0.8255		0.7973	X8	0.7400	0.7400	0.7400	0.7400	0.7401	0.7400	0.7498	
		3	0.9162	0.9162	0.9161	0.9162	0.9161	0.9161		0.8683		0.9058	0.9058	0.9058	0.9058	0.9058	0.9060	0.9058	0.8904
		4	0.9238	0.9238	0.9234	0.9240	0.9235	0.9239		0.8953		0.9329	0.9328	0.9304	0.9321	0.9353	0.9364	0.9353	0.9099
5		0.9524	0.9525	0.9512	0.9526	0.9516	0.9522	0.9124	0.9533	0.9529		0.9482	0.9522	0.9469	0.9532	0.9469	0.9299		
6		0.9628	0.9621	0.9613	0.9627	0.9613	0.9620	0.9231	0.9656	0.9641		0.9613	0.9653	0.9604	0.9649	0.9649	0.9366		
7		0.9642	0.9655	0.9630	0.9642	0.9633	0.9645	0.8546	0.9706	0.9695		0.9686	0.9705	0.9690	0.9705	0.9705	0.9449		
8		0.9767	0.9768	0.9725	0.9770	0.9734	0.9765	0.9415	0.9775	0.9770		0.9721	0.9763	0.9727	0.9727	0.9759	0.9579		
9		0.9808	0.9805	0.9786	0.9811	0.9781	0.9801	0.9608	0.9811	0.9802		0.9763	0.9807	0.9761	0.9806	0.9806	0.9635		
10		0.9833	0.9831	0.9806	0.9827	0.9807	0.9821	0.8743	0.9845	0.9829		0.9788	0.9839	0.9777	0.9833	0.9833	0.9563		
15		0.9915	0.9912	0.9877	0.9912	0.9874	0.9902	0.9722	0.9884	0.9885		0.9835	0.9877	0.9857	0.9875	0.9875	0.9787		
20		0.9943	0.9937	0.9914	0.9944	0.9901	0.9927	0.9851	0.9927	0.9909		0.9882	0.9923	0.9871	0.9901	0.9901	0.9825		
30		0.9965	0.9963	0.9935	0.9964	0.9936	0.9948	0.9906	0.9957	0.9951		0.9934	0.9957	0.9927	0.9940	0.9940	0.9898		
X3		2	0.7356	0.7356	0.7356	0.7356	0.7356	0.7356	0.5969	X9		0.8256	0.8256	0.8256	0.8256	0.8256	0.8256	0.8213	
		3	0.8023	0.8020	0.8026	0.8023	0.8022	0.8023	0.5878			0.9151	0.9151	0.9151	0.9151	0.9151	0.9151	0.9090	
		4	0.8804	0.8791	0.8802	0.8790	0.8810	0.8802	0.7837			0.9518	0.9518	0.9516	0.9518	0.9516	0.9518	0.9344	
	5	0.9120	0.9127	0.9199	0.9102	0.9189	0.9090	0.6624	0.9590		0.9589	0.9577	0.9588	0.9581	0.9587	0.9489			
	6	0.9596	0.9569	0.9608	0.9596	0.9595	0.9595	0.9099	0.9724		0.9724	0.9719	0.9724	0.9719	0.9721	0.9557			
	7	0.9648	0.9643	0.9700	0.9649	0.9689	0.9641	0.9148	0.9782		0.9782	0.9772	0.9782	0.9771	0.9781	0.9667			
	8	0.9776	0.9740	0.9802	0.9768	0.9799	0.9758	0.9348	0.9819		0.9824	0.9809	0.9822	0.9803	0.9823	0.9695			
	9	0.9838	0.9809	0.9842	0.9838	0.9844	0.9836	0.9398	0.9855		0.9850	0.9837	0.9854	0.9831	0.9847	0.9728			
	10	0.9859	0.9852	0.9867	0.9856	0.9869	0.9853	0.9572	0.9878		0.9879	0.9861	0.9878	0.9860	0.9876	0.9726			
	15	0.9908	0.9912	0.9926	0.9899	0.9927	0.9904	0.9753	0.9928		0.9930	0.9923	0.9919	0.9918	0.9910	0.9833			
	20	0.9931	0.9941	0.9954	0.9927	0.9954	0.9925	0.9811	0.9952		0.9952	0.9942	0.9945	0.9938	0.9932	0.9899			
	30	0.9962	0.9969	0.9973	0.9957	0.9974	0.9958	0.9903	0.9971		0.9969	0.9959	0.9967	0.9963	0.9961	0.9939			
	X4	2	0.7787	0.7787	0.7787	0.7764	0.7787	0.7787	0.5612		X10	0.8216	0.8216	0.8216	0.8217	0.8216	0.8217	0.7915	

	3	0.8813	0.8813	0.8813	0.8813	0.8813	0.8058		0.9115	0.9115	0.9115	0.9115	0.9115	0.9115	0.8726
	4	0.9368	0.9369	0.9368	0.9369	0.9359	0.9361	0.8656	0.9411	0.9414	0.9414	0.9417	0.9418	0.9413	0.9071
	5	0.9542	0.9539	0.9518	0.9542	0.9522	0.9542	0.9091	0.9603	0.9603	0.9595	0.9603	0.9595	0.9602	0.9130
	6	0.9662	0.9662	0.9634	0.9661	0.9637	0.9657	0.9155	0.9705	0.9707	0.9693	0.9710	0.9691	0.9705	0.9291
	7	0.9725	0.9727	0.9706	0.9726	0.9691	0.9703	0.9276	0.9757	0.9761	0.9739	0.9754	0.9732	0.9753	0.9345
	8	0.9756	0.9758	0.9731	0.9755	0.9720	0.9748	0.9368	0.9796	0.9803	0.9785	0.9799	0.9788	0.9789	0.9524
	9	0.9781	0.9773	0.9747	0.9753	0.9758	0.9771	0.9468	0.9839	0.9842	0.9827	0.9839	0.9820	0.9828	0.9544
	10	0.9804	0.9800	0.9771	0.9800	0.9773	0.9788	0.9523	0.9876	0.9870	0.9842	0.9874	0.9845	0.9864	0.9621
	15	0.9874	0.9864	0.9836	0.9872	0.9815	0.9865	0.9675	0.9925	0.9922	0.9910	0.9923	0.9913	0.9903	0.9685
	20	0.9903	0.9892	0.9875	0.9896	0.9845	0.9885	0.9735	0.9953	0.9944	0.9934	0.9950	0.9939	0.9935	0.9829
	30	0.9922	0.9909	0.9899	0.9918	0.9898	0.9912	0.9849	0.9961	0.9961	0.9956	0.9961	0.9942	0.9954	0.9909
X5	2	0.8627	0.8627	0.8627	0.8627	0.8627	0.8627	0.8491	X11	0.8247	0.8247	0.8247	0.8247	0.8247	0.8201
	3	0.9311	0.9311	0.9311	0.9311	0.9311	0.8950			0.8994	0.8994	0.8995	0.8994	0.8994	0.8929
	4	0.9368	0.9366	0.9363	0.9370	0.9363	0.9374	0.7296		0.9381	0.9379	0.9377	0.9381	0.9375	0.9380
	5	0.9404	0.9402	0.9403	0.9410	0.9417	0.9368	0.8291		0.9542	0.9539	0.9533	0.9539	0.9532	0.9538
	6	0.9589	0.9565	0.9575	0.9581	0.9548	0.9569	0.9327		0.9638	0.9635	0.9631	0.9636	0.9628	0.9636
	7	0.9652	0.9636	0.9611	0.9635	0.9600	0.9617	0.9418		0.9708	0.9706	0.9694	0.9708	0.9697	0.9572
	8	0.9723	0.9713	0.9657	0.9719	0.9678	0.9691	0.9481		0.9766	0.9764	0.9748	0.9763	0.9751	0.9764
	9	0.9737	0.9740	0.9687	0.9739	0.9682	0.9714	0.7643		0.9809	0.9808	0.9781	0.9808	0.9777	0.9798
	10	0.9739	0.9733	0.9699	0.9712	0.9684	0.9713	0.9614		0.9834	0.9817	0.9831	0.9811	0.9828	0.9700
	15	0.9815	0.9822	0.9798	0.9797	0.9788	0.9785	0.9708		0.9906	0.9897	0.9875	0.9905	0.9877	0.9893
	20	0.9849	0.9850	0.9847	0.9835	0.9845	0.9828	0.9772		0.9931	0.9936	0.9921	0.9923	0.9916	0.9916
	30	0.9872	0.9868	0.9866	0.9863	0.9870	0.9856	0.9841		0.9951	0.9949	0.9941	0.9944	0.9941	0.9932
X6	2	0.7549	0.7549	0.7549	0.7549	0.7549	0.7549	0.7461	X12	0.6720	0.6720	0.6720	0.6720	0.6720	0.3302
	3	0.8863	0.8863	0.8863	0.8863	0.8862	0.8863	0.8712		0.7837	0.7837	0.7837	0.7837	0.7837	0.4418
	4	0.9131	0.9131	0.9129	0.9131	0.9130	0.9131	0.8925		0.8514	0.8482	0.8518	0.8510	0.8518	0.8502
	5	0.9281	0.9282	0.9263	0.9275	0.9269	0.9288	0.8965		0.8710	0.8713	0.8777	0.8710	0.8757	0.8705
	6	0.9318	0.9354	0.9333	0.9305	0.9302	0.9343	0.9061		0.8975	0.8994	0.9190	0.8972	0.9180	0.8972
	7	0.9303	0.9359	0.9320	0.9282	0.9318	0.9251	0.9006		0.9661	0.9524	0.9708	0.9575	0.9627	0.9423
	8	0.9399	0.9397	0.9323	0.9357	0.9357	0.9331	0.9260		0.9688	0.9824	0.9837	0.9804	0.9837	0.9828
	9	0.9441	0.9429	0.9370	0.9422	0.9394	0.9395	0.9219		0.9864	0.9853	0.9863	0.9864	0.9864	0.9858
	10	0.9493	0.9482	0.9454	0.9467	0.9420	0.9425	0.9311		0.9881	0.9879	0.9886	0.9893	0.9882	0.9894
	15	0.9560	0.9554	0.9538	0.9547	0.9481	0.9532	0.9462		0.9939	0.9935	0.9934	0.9936	0.9936	0.9920
	20	0.9587	0.9588	0.9566	0.9575	0.9566	0.9564	0.9523		0.9959	0.9960	0.9957	0.9957	0.9956	0.9950
	30	0.9607	0.9604	0.9589	0.9602	0.9590	0.9594	0.9571		0.9975	0.9972	0.9968	0.9972	0.9971	0.9964

Bold value indicates the best value.

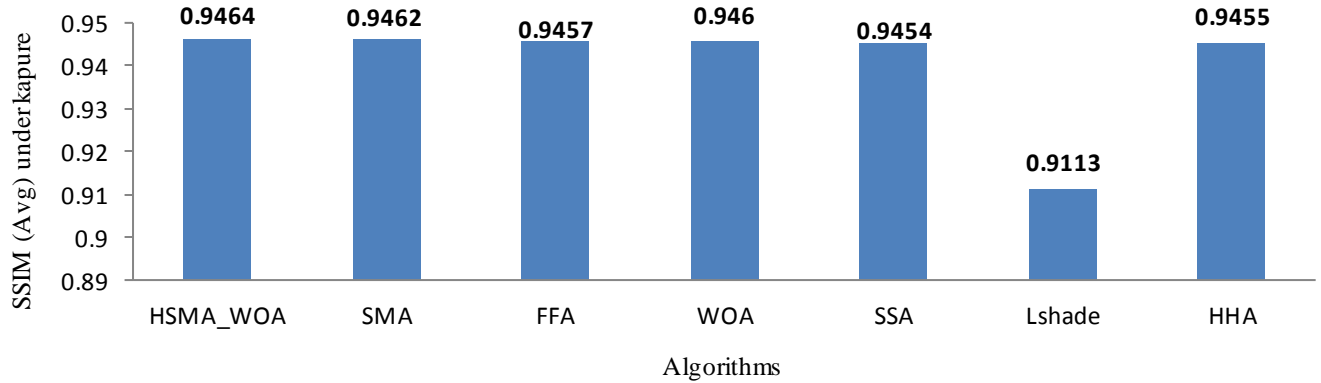


Fig.7 Average SSIM values obtained under Kapure's entropy

7.5 Universal Quality Index (UQI)

UQI [62] is an indicator similar to SSIM in measuring the quality of the segmented image based on the similarity structure between the two images rather than the error rate and mathematically formulated as in Eq. 24.

$$UQI(O, S) = \frac{(4\sigma_{os} + \mu_o\mu_s)}{(\mu_o^2 + \mu_s^2)(\sigma_o^2 + \sigma_s^2)} \quad (28)$$

where O refers to the original image, S is the segmented image, μ_o are the mean intensities of the original image, μ_s are the mean intensities of the and segmented image. σ_o and σ_s are the standard deviations for both the source and predicted image; σ_{os} is the covariance between the separated and source image. A higher value of UQI indicates better results.

After executing each algorithm, 20 runs and calculated the average UQI within them obtained by each one under Kapure's entropy, it is introduced in Table 5. By observing outcomes in this table, we notify that HSMA_WOA could overcome the others in 58 cases and equal in 20 others. In the same context, SMA could achieve the best in 18 and equal in 19. Specifically, the proposed algorithms could be superior and equal in 101 out of 144 test cases. Based on that, the proposed algorithms are competitive with others for generating a better-segmented image. In order to illustrate the data in Table 6, Fig.8 is taken to show the average UQI obtained by the algorithms within 20 runs and all the test images and threshold levels. This figure shows the superiority of the comparison of the proposed algorithms with the others under Kapur's method.

Table 6: UQI values under Kapur's entropy.

img	T	HSMA_WOA	SMA	FFA [39]	WOA [33]	SSA [60]	HHA [38]	LShade [59]	Img	HSMA_WOA	SMA	FFA [39]	WOA [33]	SSA [60]	HHA [38]	LShade [59]
X1	2	0.7479	0.7479	0.7478	0.7477	0.7479	0.7479	0.7262	X7	0.8641	0.8729	0.8729	0.8641	0.8729	0.8729	0.8647
	3	0.8760	0.8760	0.8761	0.8760	0.8760	0.8764	0.8590		0.9042	0.9042	0.9042	0.9042	0.9042	0.9042	0.8844
	4	0.9260	0.9259	0.9263	0.9258	0.9264	0.9255	0.9004		0.9380	0.9383	0.9379	0.9380	0.9379	0.9383	0.9126
	5	0.9538	0.9537	0.9553	0.9539	0.9550	0.9536	0.9285		0.9590	0.9593	0.9582	0.9590	0.9583	0.9590	0.9438
	6	0.9671	0.9668	0.9681	0.9669	0.9661	0.9666	0.9378		0.9673	0.9672	0.9662	0.9675	0.9665	0.9671	0.9398
	7	0.9752	0.9727	0.9742	0.9755	0.9755	0.9738	0.9512		0.9700	0.9718	0.9698	0.9697	0.9692	0.9701	0.9571
	8	0.9758	0.9777	0.9796	0.9765	0.9794	0.9760	0.9583		0.9734	0.9732	0.9713	0.9734	0.9721	0.9722	0.9583
	9	0.9804	0.9796	0.9831	0.9800	0.9827	0.9792	0.9670		0.9757	0.9745	0.9727	0.9756	0.9734	0.9752	0.9610
	10	0.9830	0.9836	0.9862	0.9832	0.9853	0.9821	0.9734		0.9776	0.9771	0.9745	0.9769	0.9745	0.9767	0.9619
	15	0.9925	0.9926	0.9931	0.9926	0.9933	0.9918	0.9838		0.9825	0.9824	0.9797	0.9824	0.9793	0.9798	0.9723
20	0.9954	0.9952	0.9955	0.9953	0.9958	0.9941	0.9908	0.9845	0.9845	0.9832	0.9842	0.9818	0.9827	0.9788		
30	0.9971	0.9974	0.9972	0.9971	0.9975	0.9964	0.9944	0.9867	0.9861	0.9854	0.9861	0.9850	0.9858	0.9841		
X2	2	0.8263	0.8263	0.8263	0.8263	0.8263	0.8263	0.7989	X8	0.7406	0.7406	0.7406	0.7406	0.7406	0.7406	0.7506
	3	0.9181	0.9181	0.9180	0.9181	0.9180	0.9180	0.8696		0.9064	0.9063	0.9065	0.9064	0.9063	0.9066	0.8912
	4	0.9248	0.9248	0.9244	0.9251	0.9244	0.9250	0.8966		0.9338	0.9337	0.9312	0.9329	0.9361	0.9372	0.9108
	5	0.9532	0.9533	0.9524	0.9534	0.9527	0.9531	0.9137		0.9541	0.9537	0.9491	0.9529	0.9478	0.9543	0.9308
	6	0.9639	0.9631	0.9627	0.9639	0.9627	0.9640	0.9243		0.9666	0.9650	0.9622	0.9662	0.9614	0.9659	0.9375
	7	0.9653	0.9666	0.9640	0.9654	0.9643	0.9656	0.9438		0.9713	0.9704	0.9695	0.9714	0.9699	0.9714	0.9457
	8	0.9781	0.9779	0.9737	0.9782	0.9746	0.9778	0.9427		0.9783	0.9779	0.9730	0.9771	0.9735	0.9767	0.9588
	9	0.9819	0.9815	0.9798	0.9822	0.9792	0.9812	0.9618		0.9820	0.9811	0.9772	0.9815	0.9770	0.9815	0.9643
	10	0.9845	0.9842	0.9817	0.9840	0.9818	0.9831	0.9647		0.9854	0.9838	0.9797	0.9848	0.9786	0.9841	0.9572
	15	0.9924	0.9923	0.9887	0.9922	0.9884	0.9913	0.9732		0.9893	0.9893	0.9844	0.9885	0.9865	0.9884	0.9796
20	0.9952	0.9947	0.9924	0.9954	0.9912	0.9936	0.9861	0.9935	0.9918	0.9890	0.9932	0.9880	0.9910	0.9834		
30	0.9975	0.9973	0.9945	0.9976	0.9946	0.9958	0.9916	0.9966	0.9959	0.9943	0.9965	0.9935	0.9949	0.9907		
X3	2	0.7345	0.7345	0.7345	0.7345	0.7345	0.7345	0.7353	X9	0.8269	0.8269	0.8269	0.8269	0.8269	0.8269	0.8227
	3	0.8029	0.8027	0.8032	0.8029	0.8029	0.8029	0.8111		0.9160	0.9160	0.9160	0.9160	0.9160	0.9160	0.9103
	4	0.8801	0.8790	0.8806	0.8790	0.8806	0.8804	0.8546		0.9528	0.9527	0.9525	0.9527	0.9525	0.9527	0.9358
	5	0.9125	0.9130	0.9202	0.9106	0.9193	0.9093	0.8676		0.9608	0.9607	0.9593	0.9605	0.9598	0.9604	0.9503
	6	0.9605	0.9576	0.9604	0.9605	0.9600	0.9603	0.9105		0.9732	0.9733	0.9730	0.9733	0.9729	0.9731	0.9569
	7	0.9653	0.9649	0.9706	0.9654	0.9695	0.9646	0.9153		0.9795	0.9794	0.9783	0.9794	0.9781	0.9794	0.9679
	8	0.9783	0.9747	0.9809	0.9775	0.9806	0.9765	0.9354		0.9833	0.9836	0.9821	0.9835	0.9815	0.9835	0.9706
	9	0.9849	0.9816	0.9849	0.9844	0.9851	0.9843	0.9404		0.9864	0.9861	0.9848	0.9864	0.9841	0.9857	0.9739
	10	0.9867	0.9860	0.9874	0.9863	0.9877	0.9861	0.9579		0.9888	0.9890	0.9871	0.9889	0.9871	0.9887	0.9738
	15	0.9916	0.9921	0.9935	0.9907	0.9936	0.9912	0.9760		0.9939	0.9941	0.9934	0.9929	0.9929	0.9921	0.9844
20	0.9940	0.9950	0.9964	0.9936	0.9963	0.9934	0.9819	0.9963	0.9962	0.9952	0.9955	0.9949	0.9942	0.9909		
30	0.9971	0.9978	0.9983	0.9967	0.9983	0.9968	0.9912	0.9981	0.9979	0.9970	0.9977	0.9973	0.9971	0.9949		
X4	2	0.7793	0.7793	0.7793	0.7770	0.7793	0.7793	0.7374	X10	0.8214	0.8214	0.8214	0.8216	0.8214	0.8217	0.7919
	3	0.8818	0.8818	0.8818	0.8818	0.8818	0.8819	0.8067		0.9120	0.9120	0.9120	0.9121	0.9120	0.9120	0.8731
	4	0.9376	0.9377	0.9376	0.9377	0.9367	0.9369	0.8665		0.9419	0.9422	0.9422	0.9425	0.9426	0.9421	0.9078
	5	0.9552	0.9548	0.9527	0.9551	0.9531	0.9551	0.9100		0.9610	0.9610	0.9602	0.9611	0.9602	0.9610	0.9137
	6	0.9670	0.9670	0.9643	0.9668	0.9646	0.9665	0.9163		0.9714	0.9715	0.9701	0.9719	0.9699	0.9714	0.9298
	7	0.9733	0.9735	0.9714	0.9734	0.9700	0.9712	0.9284		0.9766	0.9769	0.9748	0.9763	0.9741	0.9762	0.9352
	8	0.9764	0.9767	0.9740	0.9764	0.9729	0.9757	0.9377		0.9805	0.9812	0.9794	0.9808	0.9797	0.9798	0.9533
	9	0.9789	0.9782	0.9756	0.9762	0.9767	0.9780	0.9477		0.9849	0.9852	0.9836	0.9849	0.9829	0.9837	0.9552

	10	0.9813	0.9808	0.9780	0.9809	0.9782	0.9797	0.9532	0.9886	0.9879	0.9852	0.9884	0.9854	0.9873	0.9629
	15	0.9883	0.9873	0.9845	0.9881	0.9824	0.9874	0.9684	0.9935	0.9932	0.9920	0.9933	0.9923	0.9913	0.9694
	20	0.9912	0.9901	0.9884	0.9905	0.9854	0.9894	0.9744	0.9963	0.9954	0.9945	0.9960	0.9949	0.9945	0.9838
	30	0.9931	0.9918	0.9908	0.9926	0.9907	0.9921	0.9857	0.9972	0.9972	0.9967	0.9971	0.9953	0.9964	0.9919
X5	2	0.8640	0.8640	0.8640	0.8640	0.8640	0.8640	0.8496	X11	0.8261	0.8261	0.8261	0.8261	0.8261	0.8213
	3	0.9314	0.9314	0.9314	0.9314	0.9314	0.9314	0.8955		0.9010	0.9010	0.9010	0.9010	0.9010	0.8939
	4	0.9371	0.9369	0.9366	0.9374	0.9368	0.9378	0.9051		0.9392	0.9391	0.9388	0.9392	0.9386	0.9391
	5	0.9410	0.9407	0.9409	0.9416	0.9424	0.9374	0.9225		0.9550	0.9548	0.9545	0.9549	0.9543	0.9547
	6	0.9595	0.9570	0.9584	0.9587	0.9556	0.9576	0.9335		0.9649	0.9646	0.9641	0.9647	0.9637	0.9647
	7	0.9659	0.9644	0.9618	0.9642	0.9608	0.9625	0.9426		0.9717	0.9715	0.9703	0.9716	0.9705	0.9716
	8	0.9731	0.9721	0.9664	0.9727	0.9687	0.9698	0.9489		0.9775	0.9774	0.9757	0.9772	0.9760	0.9773
	9	0.9745	0.9748	0.9695	0.9746	0.9690	0.9722	0.9539		0.9819	0.9817	0.9790	0.9818	0.9787	0.9807
	10	0.9746	0.9741	0.9706	0.9720	0.9692	0.9721	0.9622		0.9843	0.9843	0.9828	0.9841	0.9821	0.9838
	15	0.9824	0.9831	0.9806	0.9805	0.9797	0.9794	0.9716		0.9913	0.9907	0.9884	0.9915	0.9887	0.9903
	20	0.9858	0.9859	0.9856	0.9844	0.9854	0.9837	0.9780		0.9940	0.9945	0.9930	0.9933	0.9926	0.9925
	30	0.9881	0.9877	0.9875	0.9872	0.9879	0.9865	0.9850		0.9960	0.9958	0.9950	0.9954	0.9950	0.9941
X6	2	0.7571	0.7571	0.7571	0.7571	0.7571	0.7571	0.7472	X12	0.6728	0.6728	0.6728	0.6728	0.6728	0.6992
	3	0.8880	0.8880	0.8880	0.8880	0.8878	0.8879	0.8724		0.7842	0.7842	0.7842	0.7842	0.7842	0.7617
	4	0.9142	0.9142	0.9140	0.9142	0.9141	0.9143	0.8934		0.8524	0.8490	0.8528	0.8520	0.8528	0.8511
	5	0.9292	0.9293	0.9274	0.9287	0.9280	0.9299	0.8977		0.8715	0.8719	0.8785	0.8715	0.8764	0.8711
	6	0.9329	0.9365	0.9344	0.9316	0.9313	0.9354	0.9071		0.8984	0.9002	0.9198	0.8980	0.9189	0.8980
	7	0.9315	0.9369	0.9330	0.9294	0.9330	0.9262	0.9017		0.9670	0.9533	0.9717	0.9584	0.9635	0.9432
	8	0.9410	0.9408	0.9335	0.9368	0.9368	0.9342	0.9271		0.9697	0.9833	0.9846	0.9813	0.9846	0.9837
	9	0.9452	0.9440	0.9381	0.9433	0.9405	0.9406	0.9230		0.9874	0.9863	0.9873	0.9874	0.9873	0.9868
	10	0.9503	0.9493	0.9464	0.9479	0.9431	0.9436	0.9321		0.9891	0.9888	0.9895	0.9902	0.9892	0.9904
	15	0.9570	0.9565	0.9548	0.9558	0.9491	0.9543	0.9472		0.9948	0.9945	0.9944	0.9945	0.9946	0.9930
	20	0.9597	0.9598	0.9577	0.9586	0.9576	0.9574	0.9534		0.9969	0.9969	0.9966	0.9967	0.9966	0.9959
	30	0.9617	0.9614	0.9599	0.9612	0.9600	0.9604	0.9581		0.9985	0.9982	0.9978	0.9982	0.9981	0.9974

The bold value indicates the best value.

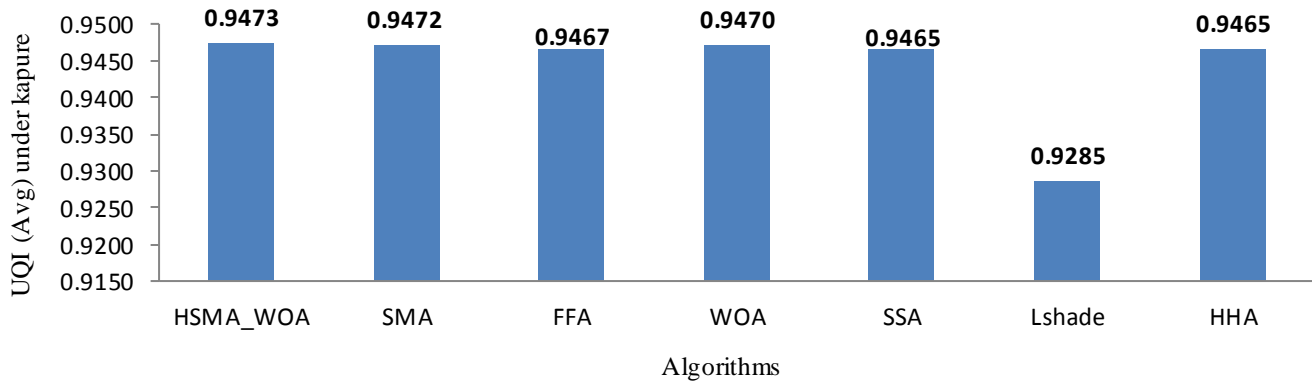
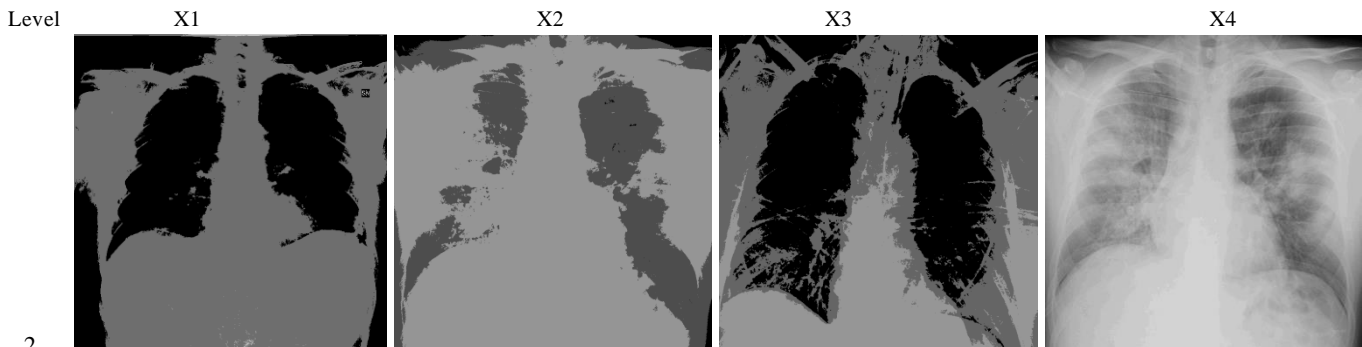
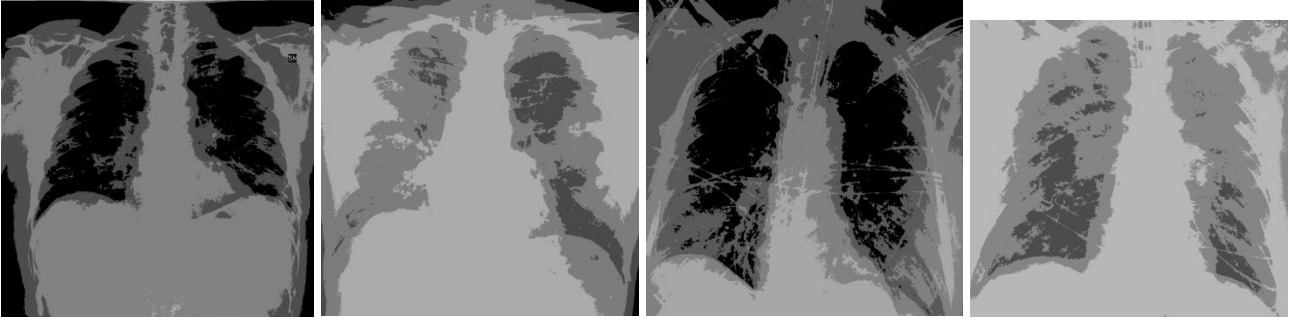


Fig.8 Average UQI values obtained under Kapur's entropy

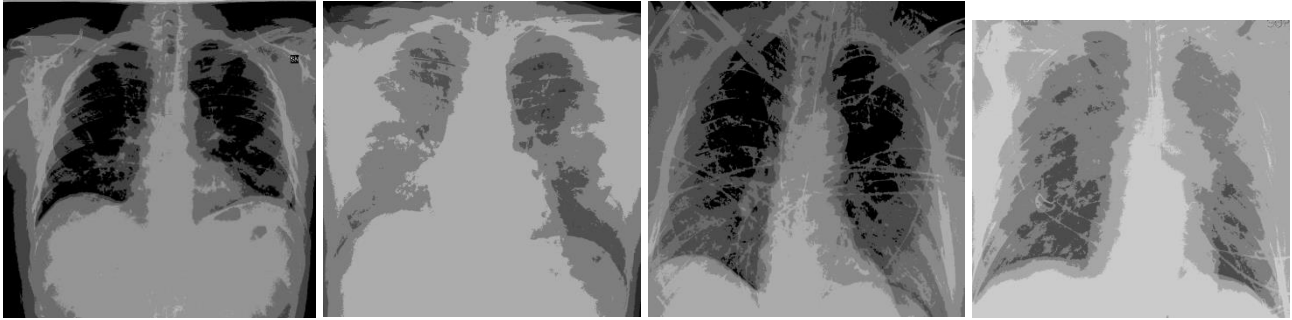
Fig.9 shows the segmented images obtained by the proposed algorithm on X1, X2, X3, and X4 under both Kapur's for the threshold levels 2, 3, 4, 5, 6, 7, 8, 9, 10, 15, 20, and 30



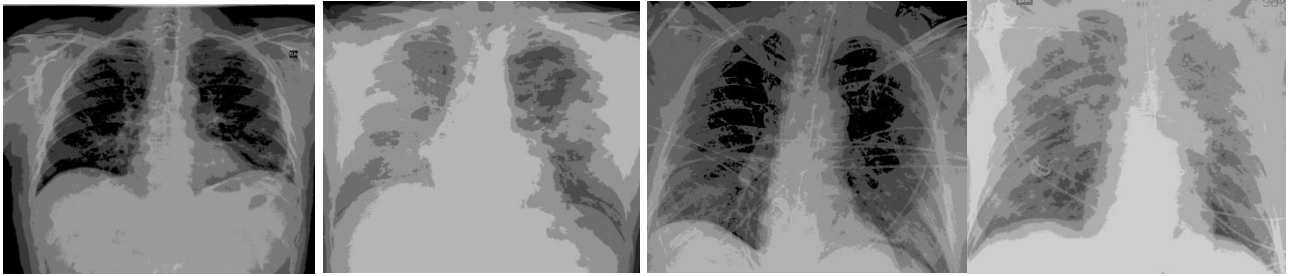
3



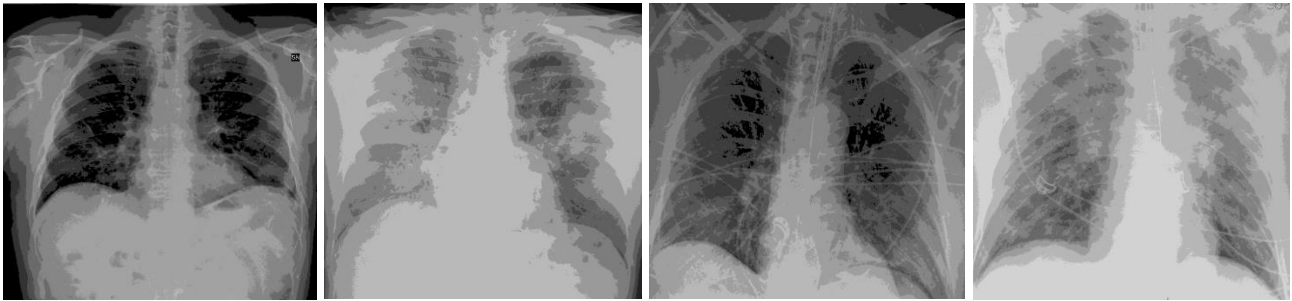
4



5



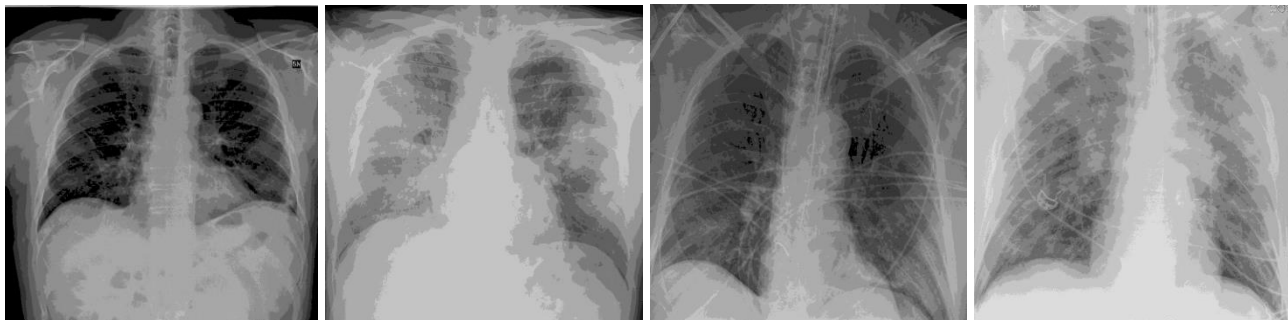
6



7



8



9



10



15



20



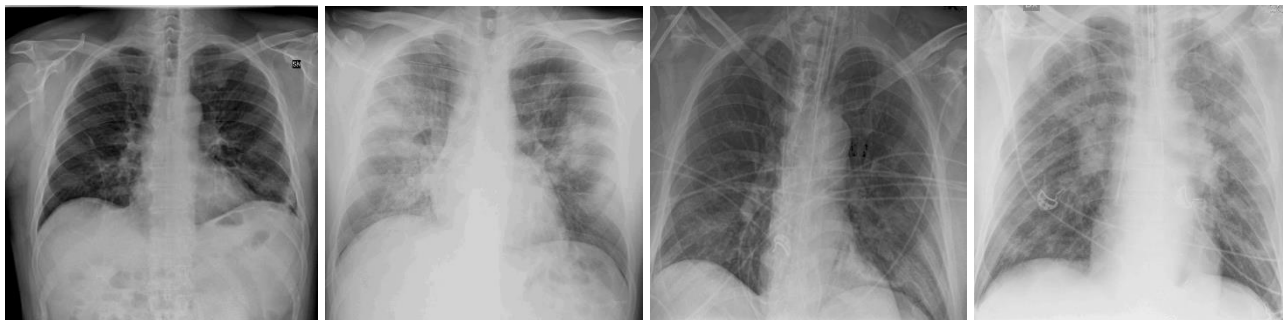


Fig.9: Segmented images by proposed algorithm under Kapure's entropy

7.8. Comparison of convergence curve among SMA, HSMA_WOA, and WOA

In this part, the convergence rate by SMA, HSMA_WOA, and WOA will be observed to illustrate the effectiveness of our approach. Generally speaking, X1, X2, X3, X4, X5, and X6 test images with 30 threshold levels are used to check the convergence rate of each algorithm. After running each algorithm, the output in each iteration on each test image from X1 to X6 is plotted in Fig.10-15, respectively. Inspecting these figures show that within the first CI=100 iteration, the convergence is accelerated as possible, but at the end of CI, the outcomes have no change and the possibility of reaching a better solution is so hard because the algorithm may be gotten stuck into local minima. As a result, it is time to integrate SMA with WOA to refresh its performance to get out of local optima, find better solutions and use the significant exploitation capability of SMA.

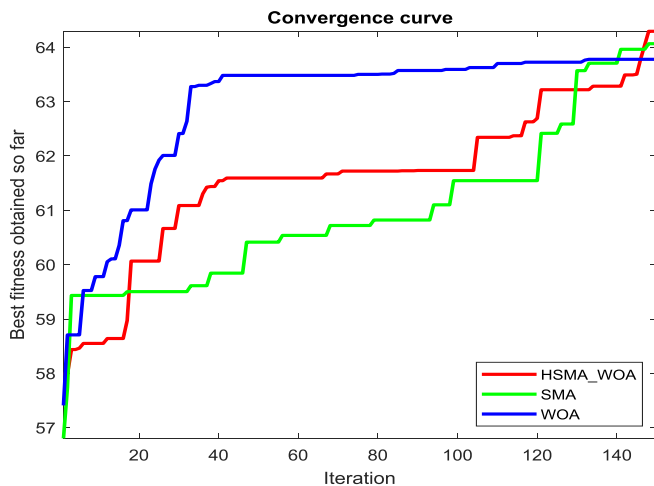


Fig.10 convergence curve on X1

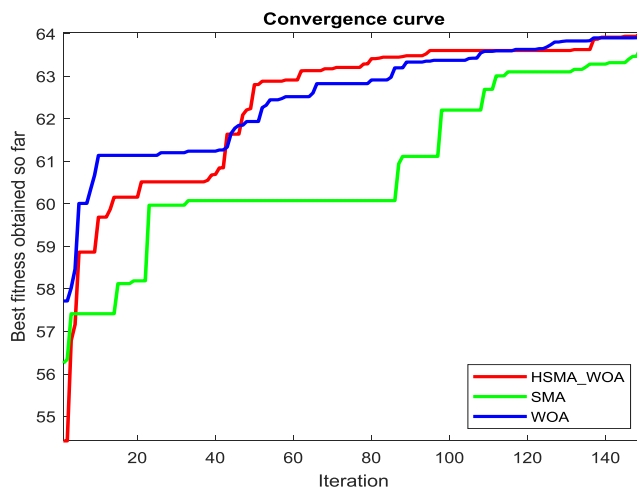


Fig.11 convergence curve on X2

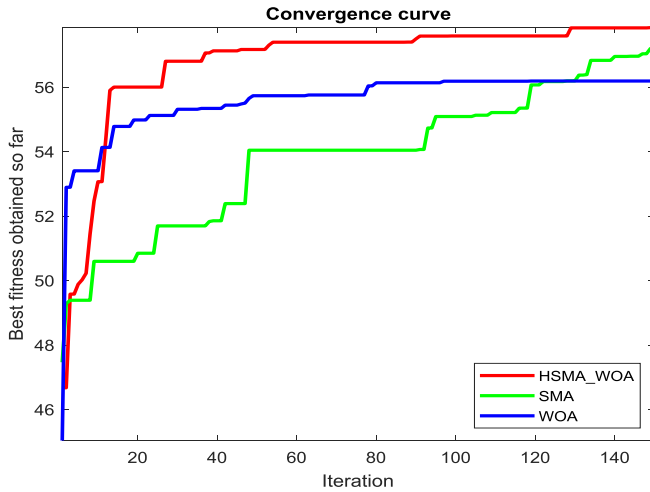


Fig.12 convergence curve on X3

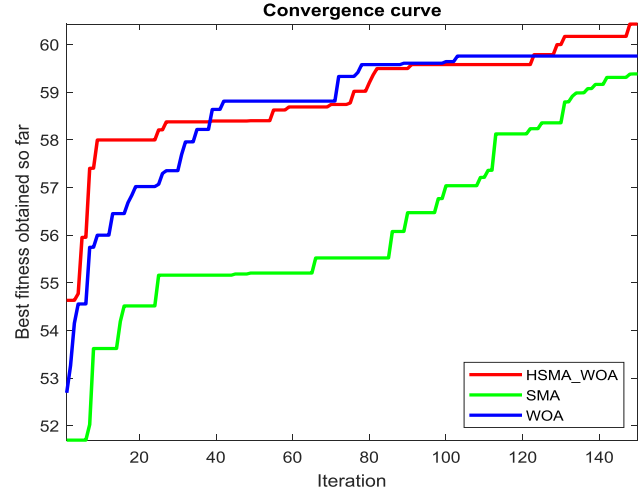


Fig.13 convergence curve on X4

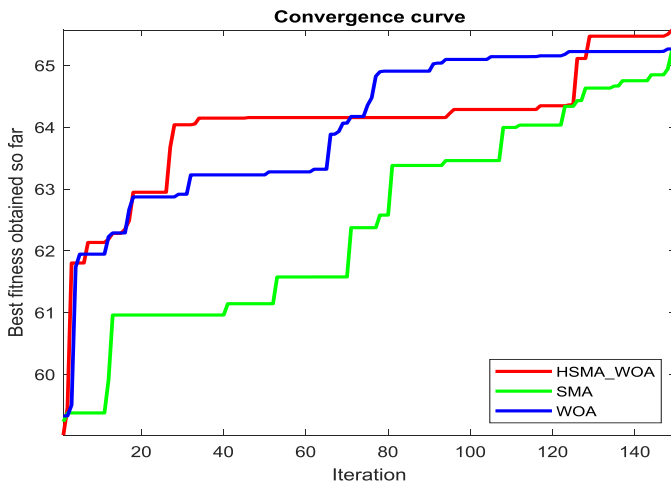


Fig.14 convergence curve on X5

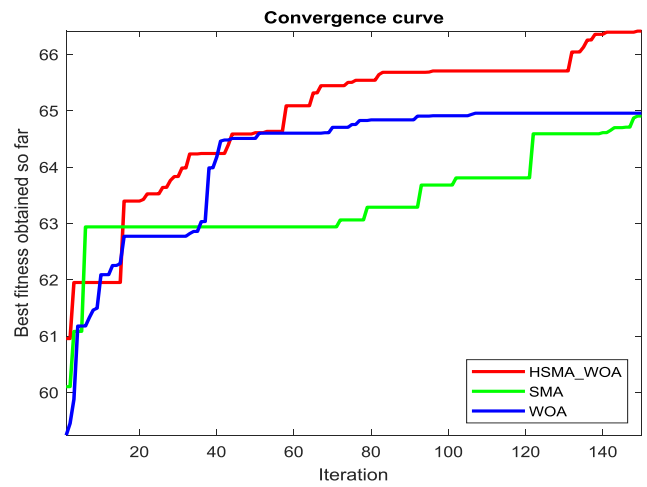


Fig.15 convergence curve on X6

8. Conclusion and Future work

According to the ongoing outbreaks of COVID-19 worldwide since December 2019, the entire world has moved to rely on technology to find tools and techniques to help identify the infected persons out of the normal ones. After many attempts and confirmed by the medical scientists, chest CT images could significantly identify whether the suspected patients have been infected. COVID-19 infection could be identified by the bilateral pulmonary parenchymal ground-glass and consolidative pulmonary opacities. Sometimes a rounded morphology and a peripheral lung distribution could be spotted. However, CT scan is so expensive compared to X-ray, and unfortunately, the specification of the infection under X-ray is so hard. The reason was that the X-ray images were considered normal images, so it could be processed using a machine learning technique to specify if this person infected or not. But when machine learning focused on the whole image, their accuracy reduced significantly. Therefore, it was necessary to find a tool to extract similar regions within the image until managing to improve the accuracy of the machine learning technique when classifying the CT images.

The process of separating or extracting the similar regions into an image was called image segmentation problem. According to that, in this paper, our techniques were based on extracting the similar small regions into chest images as an attempt to extract the regions that may contain COVID-19, and this process was known as image segmentation problem (ISP). Several techniques were proposed for tackling ISP. A technique called threshold-based segmentation was distinguished from involving those techniques with its simplicity, speed, and accuracy when segmenting an image. Hence, a new hybrid multi-thresholding approach based on the SMA behavior with WOA for overcoming ISP was proposed in this paper. Its effectiveness was observed with five state-of-art algorithms such as WOA, SSA, Lshade, HHA, and FFA. The comparison was performed by applying the algorithms on a set of chest X-ray images with threshold levels between 2 and 30. Based on the results obtained by each algorithm, the performance of the proposed algorithm was verified to outperform all other algorithms in the fitness values, SSIM, PSNR, UQI, CPU time and (Std).

With rapidly-increased reported cases worldwide and the need to verify our algorithm with new images, the future work will involve validating the performance of the proposed algorithm on a set of the test images taken from The Berkeley Segmentation Dataset and Benchmark. The aim will be focused on checking whether its performance is stable on the other images. Furthermore, the improved Slime mould algorithm will be applied to solve flow shop scheduling problems, DNA fragment assembly problems, and parameter estimation of the photovoltaic solar cell.

Acknowledgment

This research is partly supported by VC Research (VCR 0000075) for Prof Chang.

References

1. Bai, Y., et al., *Presumed asymptomatic carrier transmission of COVID-19*. *Jama*, 2020. **323**(14): p. 1406-1407.
2. Guan, C.S., et al., *Imaging Features of Coronavirus disease 2019 (COVID-19): Evaluation on Thin-Section CT*. *Academic Radiology*, 2020.
3. Kuruvilla, J., et al. *A review on image processing and image segmentation*. in *2016 international conference on data mining and advanced computing (SAPIENCE)*. 2016. IEEE.
4. Hu, R., et al., *Utilizing large scale vision and text datasets for image segmentation from referring expressions*. arXiv preprint arXiv:1608.08305, 2016.
5. Mittal, M., et al., *Image Segmentation Using Deep Learning Techniques in Medical Images*, in *Advancement of Machine Intelligence in Interactive Medical Image Analysis*. 2020, Springer. p. 41-63.
6. Zhang, Z., et al., *DENSE-INception U-net for medical image segmentation*. *Computer Methods and Programs in Biomedicine*, 2020: p. 105395.
7. Wang, X., X. Wang, and D.M. Wilkes, *An Efficient Image Segmentation Algorithm for Object Recognition Using Spectral Clustering*, in *Machine Learning-based Natural Scene Recognition for Mobile Robot Localization in An Unknown Environment*. 2020, Springer. p. 215-234.
8. Karydas, C.G., *Optimization of multi-scale segmentation of satellite imagery using fractal geometry*. *International Journal of Remote Sensing*, 2020. **41**(8): p. 2905-2933.

9. Su, T. and S. Zhang, *Local and global evaluation for remote sensing image segmentation*. ISPRS Journal of Photogrammetry and Remote Sensing, 2017. **130**: p. 256-276.
10. Alberti, M., et al. *Historical document image segmentation with LDA-initialized deep neural networks*. in *Proceedings of the 4th International Workshop on Historical Document Imaging and Processing*. 2017.
11. Naoum, A., J. Nothman, and J. Curran. *Article segmentation in digitised newspapers with a 2D Markov model*. in *2019 International Conference on Document Analysis and Recognition (ICDAR)*. 2019. IEEE.
12. Barman, R., et al., *Combining Visual and Textual Features for Semantic Segmentation of Historical Newspapers*. arXiv preprint arXiv:2002.06144, 2020.
13. Aksac, A., T. Ozyer, and R. Alhaji, *Complex networks driven salient region detection based on superpixel segmentation*. Pattern Recognition, 2017. **66**: p. 268-279.
14. Prathusha, P. and S. Jyothi, *A Novel edge detection algorithm for fast and efficient image segmentation*, in *Data Engineering and Intelligent Computing*. 2018, Springer. p. 283-291.
15. Narayanan, B.N., et al., *Optimized feature selection-based clustering approach for computer-aided detection of lung nodules in different modalities*. Pattern Analysis and Applications, 2019. **22**(2): p. 559-571.
16. Han, J., et al., *A new multi-threshold image segmentation approach using state transition algorithm*. Applied Mathematical Modelling, 2017. **44**: p. 588-601.
17. Oliva, D., et al., *A multilevel thresholding algorithm using electromagnetism optimization*. Neurocomputing, 2014. **139**: p. 357-381.
18. Arora, S., et al., *Multilevel thresholding for image segmentation through a fast statistical recursive algorithm*. Pattern Recognition Letters, 2008. **29**(2): p. 119-125.
19. Dirami, A., et al., *Fast multilevel thresholding for image segmentation through a multiphase level set method*. Signal Processing, 2013. **93**(1): p. 139-153.
20. Kapur, J.N., PK Sahoo, and A.K. Wong, *A new method for gray-level picture thresholding using the entropy of the histogram*. Computer vision, graphics, and image processing, 1985. **29**(3): p. 273-285.
21. Oliva, D., M.A. Elaziz, and S. Hinojosa, *Fuzzy entropy approaches for image segmentation*, in *Metaheuristic Algorithms for Image Segmentation: Theory and Applications*. 2019, Springer. p. 141-147.
22. Abdel-Basset, M., et al., *A hybrid whale optimization algorithm based on local search strategy for the permutation flow shop scheduling problem*. Future Generation Computer Systems, 2018. **85**: p. 129-145.
23. Sayed, G.I., A.E. Hassanien, and A.T. Azar, *Feature selection via a novel chaotic crow search algorithm*. Neural Computing and Applications, 2019. **31**(1): p. 171-188.
24. Rizk-Allah, R.M., et al., *A new binary salp swarm algorithm: development and application for optimization tasks*. Neural Computing and Applications, 2019. **31**(5): p. 1641-1663.
25. Cuevas, E., J. Gálvez, and O. Avalos, *An Enhanced Crow Search Algorithm Applied to Energy Approaches*, in *Recent Metaheuristics Algorithms for Parameter Identification*. 2020, Springer. p. 27-49.
26. Cuevas, E., F. Fausto, and A. González, *The Locust Swarm Optimization Algorithm*, in *New Advancements in Swarm Algorithms: Operators and Applications*. 2020, Springer. p. 139-159.
27. Ibrahim, R.A., et al., *An opposition-based social spider optimization for feature selection*. Soft Computing, 2019. **23**(24): p. 13547-13567.
28. Guo, C. and H. Li. *Multilevel thresholding method for image segmentation based on an adaptive particle swarm optimization algorithm*. in *Australasian joint conference on artificial intelligence*. 2007. Springer.
29. Xiong, L., et al., *Color disease spot image segmentation algorithm based on chaotic particle swarm optimization and FCM*. The Journal of Supercomputing, 2020: p. 1-15.
30. Di Martino, F. and S. Sessa, *PSO image thresholding on images compressed via fuzzy transforms*. Information Sciences, 2020. **506**: p. 308-324.
31. Kaveh, A. and S. Talatahari, *An improved ant colony optimization for constrained engineering design problems*. Engineering Computations, 2010. **27**(1): p. 155-182.
32. Huo, F., X. Sun, and W. Ren, *Multilevel image threshold segmentation using an improved Bloch quantum artificial bee colony algorithm*. Multimedia Tools and Applications, 2020. **79**(3): p. 2447-2471.
33. El Aziz, MA, A.A. Ewees, and A.E. Hassanien, *Whale optimization algorithm and moth-flame optimization for multilevel thresholding image segmentation*. Expert Systems with Applications, 2017. **83**: p. 242-256.

34. Elsayed, SM, RA Sarker, and DL Essam, *A new genetic algorithm for solving optimization problems*. Engineering Applications of Artificial Intelligence, 2014. **27**: p. 57-69.
35. Kandhway, P. and A.K. Bhandari, *Spatial context cross entropy function based multilevel image segmentation using multi-verse optimizer*. Multimedia Tools and Applications, 2019. **78**(16): p. 22613-22641.
36. Agrawal, S., et al., *Tsallis entropy based optimal multilevel thresholding using cuckoo search algorithm*. Swarm and Evolutionary Computation, 2013. **11**: p. 16-30.
37. Chakraborty, F., D. Nandi, and P.K. Roy, *Oppositional symbiotic organisms search optimization for multilevel thresholding of color image*. Applied Soft Computing, 2019: p. 105577.
38. Bao, X., H. Jia, and C. Lang, *A Novel Hybrid Harris Hawks Optimization for Color Image Multilevel Thresholding Segmentation*. IEEE Access, 2019. **7**: p. 76529-76546.
39. Erdmann, H., et al., *A study of a firefly meta-heuristics for multithreshold image segmentation*, in *Developments in medical image processing and computational vision*. 2015, Springer. p. 279-295.
40. Wang, R., et al., *A hybrid flower pollination algorithm based modified randomized location for multi-threshold medical image segmentation*. Bio-medical materials and engineering, 2015. **26**(s1): p. S1345-S1351.
41. Oliva, D., et al., *Cross entropy based thresholding for magnetic resonance brain images using Crow Search Algorithm*. Expert Systems with Applications, 2017. **79**: p. 164-180.
42. Yao, X., et al. *Multi-Threshold Image Segmentation Based on Improved Grey Wolf Optimization Algorithm*. in *IOP Conference Series: Earth and Environmental Science*. 2019. IOP Publishing.
43. Horng, M.-H., *Multilevel minimum cross entropy threshold selection based on the honey bee mating optimization*. Expert Systems with Applications, 2010. **37**(6): p. 4580-4592.
44. Cuevas, E., F. Fausto, and A. González, *Locust Search Algorithm Applied to Multi-threshold Segmentation*, in *New Advancements in Swarm Algorithms: Operators and Applications*, E. Cuevas, F. Fausto, and A. González, Editors. 2020, Springer International Publishing: Cham. p. 211-240.
45. Singla, A. and S. Patra, *A fast automatic optimal threshold selection technique for image segmentation*. Signal Image & Video Processing, **11**: 1-8. 2016.
46. Manikandan, S., et al., *Multilevel thresholding for segmentation of medical brain images using real coded genetic algorithm*. Measurement, 2014. **47**: p. 558-568.
47. Maitra, M. and A. Chatterjee, *A hybrid cooperative-comprehensive learning based PSO algorithm for image segmentation using multilevel thresholding*. Expert Systems with Applications, 2008. **34**(2): p. 1341-1350.
48. Liu, Y., et al., *Modified particle swarm optimization-based multilevel thresholding for image segmentation*. Soft computing, 2015. **19**(5): p. 1311-1327.
49. Ghamisi, P., et al., *Multilevel image segmentation based on fractional-order Darwinian particle swarm optimization*. IEEE Transactions on Geoscience and Remote sensing, 2013. **52**(5): p. 2382-2394.
50. Chen, K., et al., *Multilevel image segmentation based on an improved firefly algorithm*. Mathematical Problems in Engineering, 2016. **2016**.
51. Bhandari, A.K., A. Kumar, and G.K. Singh, *Modified artificial bee colony based computationally efficient multilevel thresholding for satellite image segmentation using Kapur's, Otsu and Tsallis functions*. Expert Systems with Applications, 2015. **42**(3): p. 1573-1601.
52. Sanyal, N., A. Chatterjee, and S. Munshi, *An adaptive bacterial foraging algorithm for fuzzy entropy based image segmentation*. Expert Systems with Applications, 2011. **38**(12): p. 15489-15498.
53. Sathya, P. and R. Kayalvizhi, *Modified bacterial foraging algorithm based multilevel thresholding for image segmentation*. Engineering Applications of Artificial Intelligence, 2011. **24**(4): p. 595-615.
54. Abdel-Basset, M., V. Chang, and R. Mohamed, *A novel equilibrium optimization algorithm for multi-thresholding image segmentation problems*. Neural Computing and Applications, 2020: p. 1-34.
55. Abdel-Basset, M., et al., *A hybrid COVID-19 detection model using an improved marine predators algorithm and a ranking-based diversity reduction strategy*. IEEE Access, 2020.
56. Chouksey, M., R.K. Jha, and R. Sharma, *A fast technique for image segmentation based on two Meta-heuristic algorithms*. Multimedia Tools and Applications, 2020: p. 1-53.

57. Mirjalili, S. and A. Lewis, *The whale optimization algorithm*. Advances in engineering software, 2016. **95**: p. 51-67.
58. Nakagaki, T., H. Yamada, and T. Ueda, *Interaction between cell shape and contraction pattern in the Physarum plasmodium*. Biophysical chemistry, 2000. **84**(3): p. 195-204.
59. Brest, J., M.S. Maučec, and B. Bošković. *iL-SHADE: Improved L-SHADE algorithm for single objective real-parameter optimization*. In *2016 IEEE Congress on Evolutionary Computation (CEC)*. 2016. IEEE.
60. Wang, S., H. Jia, and X. Peng, *Modified salp swarm algorithm based multilevel thresholding for color image segmentation*. Mathematical biosciences and engineering: MBE, 2019. **17**(1): p. 700-724.
61. Hore, A. and D. Ziou. *Image quality metrics: PSNR vs. SSIM*. In *2010 20th International Conference on Pattern Recognition*. 2010. IEEE.
62. Egiazarian, K., et al. *New full-reference quality metrics based on HVS*. in *Proceedings of the Second International Workshop on Video Processing and Quality Metrics*. 2006.